6-2007

Experimental Investigation and Numerical Modeling of Hybrid Glass/Carbon FRP Section Combined with Concrete Slab

Stephen Craig Raynor

United Arab Emirates University

Deanship of Graduate Studies

Experimental Investigation and Numerical Modeling of Hybrid Glass/Carbon FRP Section Combined with Concrete Slab

By

Stephen C Raynor, B.E (Civil) (Honours)

Supervised by

Dr. Ashraf Biddah
Civil & Env. Engineering Department
College of Engineering,
UAE University

Dr. Khaled El-Sawy
Civil & Env. Engineering Department
College of Engineering,
UAE University

Submitted to the Deanship of Graduate Studies in partial fulfilment of the requirements for the degree of Master of Science in Materials Science and Engineering

June 2007

ACKNOWLEDGEMENTS

I would like to express my gratitude and appreciation to Dr Ashraf Biddah and Dr Khalid El-Sawy of the United Arab Emirates University Civil & Environmental Engineering Department for their constant patience and happy "nice to hear from you" whatever hour I called. Your guidance and advice, support and sharp observations motivated a far greater learning than I could have otherwise hoped for.

Thanks also to the UAEU for their confidence in my ability to successfully complete the Masters of Science in Materials Engineering study when selecting me for the program.

People who have provided equipment and supplies time and effort, thanks to you also. In particular De Gussa, the suppliers of the expensive carbon fibre related elements and the civil laboratory staff at United Arab Emirates University

Finally this thesis is dedicated to my wife and children who suffered the joys and disappointments along with me as the research sometimes crept and sometimes sped towards completion. Their care and sacrifice made it possible.

TABLE OF CONTENTS

LIST OF TABLES

Chapter Three

Chapter Four

LIST OF FIGURES

Chapter Three

Chapter Four

CHAPTER ONE: INTRODUCTION

CHAPTER ONE: INTRODUCTION

1.1 General Overview

There are many engineering applications that would require the design and construction of lightweight, corrosion resistant, yet inexpensive structures suitable for use in harsh environments. These engineering applications include onshore, marine and offshore structures in which the use of traditional reinforced concrete (RC) and/or steel structures typically requires costly regular maintenance throughout the life span of the structures. This need has directed many researchers to explore alternative solutions rather than using RC or steel structures. The study presented herein is an attempt in this direction. The study considers only flexural structural members that are basic components in almost any structural system.

1.2 Fibre Reinforced Polymer Composites as Structural Materials

Fibre reinforced polymer composite (FRP) is manufactured from strong fibres acting within a matrix of polymer or plastic. This creates a material that is very strong and moderately stiff along the fibre direction and with less stiffness and strength in all the other directions. Due to the rapidly growing use of FRP in the civil construction industry worldwide, it is thought that such material, with its high tensile strength, light weight, ease of handling and corrosion resistance, would represent a valid candidate to be considered in this study.

Historically, FRP composites have been the material of choice in the aerospace industry since 1960. However, only recently glass FRP (GFRP) composites have been gaining acceptance as a structural material. More recently carbon FRP (CFRP) has also become cost competitive and offers even higher structural properties than GFRP. However, deformability and high cost of FRP remain obstacles to more widespread use. To overcome these disadvantages, previous studies have proposed structural elements in which GFRP is combined with other less expensive structural materials. For example GFRP rods have been proposed as reinforcing bars for concrete. CFRP plates have been bonded to external surfaces of reinforced concrete structures as repair or strengthening measures. More recently testing with Pultruded GFRP sections working in composite action with a concrete slab have produced positive results in terms of load and deflection criteria.

Studies of the use of FRP with concrete have focused frequently on the use of FRP elements as strengthening or retrofitting solutions rather than an integral component of the design of the structural member. Recently, in the work by Biddah (2003), he has begun to experiment with the use of FRP as an integral design element of the beams. The benefits offered by this method are light weight structures and good resistance to the corrosive elements in the UAE and other harsh environments.

1.3 Composite Action and its Benefits in Beams

Composite action is a term applied to structures or structural elements that are made of two or more sub elements which are connected in such a manner that causes the sub elements to act together as fully or partially integrated single element. Composite action is desirable to provide longer spans and lower deflections for beams

The structural behaviour of a composite structural beam is largely dependant on the amount of composite action achieved. Achieving composite action is dependant on shear forces being adequately transferred between the different sub-elements. A fully rigid connection will usually develop full composite action between the individual sub-elements. Flexible shear connectors will only permit development of partial composite action and what is termed "slip" will occur across the interface between the sub elements. Rigid connectors include heavy steel bars and rigid adhesives. Flexible connectors include steel studs, bolts and nail plates.

In this research the term hybrid composite is used to describe the multitude of composite actions taking place in the beams under study. A well known example of composite beams is the steel I- or channel beam with concrete slab connected to the top flange of the beam. In that configuration, the concrete slab works as a compression flange for the beam while the steel section (I or channel section) mainly carries the tension and shear applied to the beam. Conventionally, studs welded to the steel beam and embedded in the concrete slab are used as shear connectors.

1.4 Proposal for a New Composite Beam Configuration

The motivation behind this study is to investigate the behaviour of a possible hybrid composite configuration of a beam capable of providing high performance, lightweight corrosion resistant structural element. Based on the previous review of the different materials and configurations, this thought of approach is to:

- use of concrete as a compressive sub-element since it is cheap and reasonably resistant to corrosion,
- use of CFRP as a high strength tension element since it is, although relatively expensive, is required in small amounts and is also corrosion resistant, and
- use of two back-to-back GFRP Channel sections to provide depth to the structural section and to carry most of the beam shear since it is relatively cheap and will resist corrosion as well as being reasonably inexpensive.

Fortunately, GFRP has been recently manufactured in standard structural shapes such as channels, angles and I sections that can be easily incorporated into a regular structure. To ensure composite action is maintained for the entire section horizontal shear connectors are installed between the concrete slab and pultruded GFRP beam. CFRP is also epoxy bonded to the underside of the GFRP beam.

1.5 Methodology and Expected Outcomes

The main two objectives of the research are to experimentally investigate the behaviour of the proposed hybrid composite configuration under flexure, and to attempt to simulate the observed behaviour numerically using the Finite Element Method. To achieve the first objective, test specimens are to be designed, manufactured and tested to failure and experimental data will be recorded and analysed for a future check against the Finite Element results. The second objective is known to be a tough job which, if fulfilled, will open the door widely for more investigation of different beam setups and configurations.

It was intended that the findings of this study be additive to the work completed by Biddah (2003) and therefore similar sections and spans were adopted. Concrete and GRFP strengths were also matched as far as possible. One area where changes were made was in the shear connections between the concrete slab and the GFRP beam. In Biddah's experimental work, 200mm centre-to-centre connecting bolts were used and resulted in buckling failure in the GFRP top flange. Therefore, in this study the shear connectors were placed more closely at 125mm longitudinal centre-to-centre spacing in an attempt to restrain the top flange sufficiently against buckling.

The effect of increasing the amount of CFRP was of interest and so the testing applied different amounts of CFRP so that these effects could be observed. It is well reported that the failure mode of beams with externally applied CFRP is de-bonding of the FRP. Methods of attachment are subject to major studies and were not a part of the study to be

undertaken here. The approach adopted was to use commercially available epoxy adhesive / CFRP combinations, the one adopted was provided by BASF.

1.6 Organisation of the Thesis

This thesis is organized into 5 chapters that describe the background, the experimental and the analytical research performed.

- Chapter 1 provides an introduction and overview to the philosophy behind the study presented in this thesis.
- Chapter 2 reviews previous work in this field and describes the experimental program and the approach to validation of the numerical model developed during the research.
- Chapter 3 follows the experimental program and reports on behaviours and failures as observed, concluding with a summary of experimental findings.
- Chapter 4 outlines the numerical model and the approach to simulating the beam behaviour numerically. This chapter concludes with a comparison of experimental and analytical results.
- Chapter 5 brings together the findings of both the experimental and analytical research and discusses the results and general conclusions arrived at from this work. Areas for future study are identified here also.

CHAPTER TWO: LITERATURE REVIEW

CHAPTER TWO: LITERATURE REVIEW

2.1 Introduction

This chapter reviews the present situation with regard to the use of FRP in civil applications and the state of research in this area of application. Aspects that have been reviewed include the use of FRP as a component in structures, the use and analysis of composite action in load carrying elements, and the use of finite element modelling component parts and entire beams.

2.2 Review of previous work

FRP as a component in structures

FRP has been used successfully in structural applications for around 2 decades now. As early as 1990 GFRP was used as a replacement for steel reinforcing bars in concrete and were being explored as a material for pre-stressing tendons in concrete piles (Sen 1990). Acceptance of FRP has now developed to the point where design guidelines for concrete structures reinforced with FRP bars have been published. For example the Canadian Highway Bridge Design Code CAN/CSA-S6-00 2000 includes a complete section on use of FRP composite reinforcing bars in concrete slabs, beams and walls.

Research into the effectiveness of FRP and concrete composites has been accelerating during this time, particularly related to the field of strengthening and retrofitting of road structures such as bridges and culverts (Yunovich and Thompson 2003).

In 2003, Biddah introduced the element of composite action between a concrete slab and a standard GFRP structural section in a simply supported single span beam. Findings of this research indicted positive benefits of composite action with a 10% reduction in deflection and more than double the load carrying capacity.

In progressing this line of research a review of literature in the fields of composite action and finite element method modelling is implied.

Composite action and shear connection literature review

Composite action is a term applied to two or more sub elements that are connected in such a manner that causes the sub elements to act together. The behaviour of such a structural member is largely dependant on the amount of composite action achieved. Achieving composite action is in turn dependant on shear forces being adequately transferred between the different sub-elements. A fully rigid connection will usually develop full composite action between the individual sub-elements. Flexible shear connectors will only permit development of partial composite action and what is termed "slip" will occur across the interface between the sub elements. The value of this slip modulus is represented as "K". Studies have been undertaken to quantify this connection and its effect on the beam for

over 60 years now and are still being undertaken in an effort to refine the design process and more recently to incorporate FRP as a new material.

Design theory for calculation of one dimensioned partial composite action subject to static loads was first developed in the 1940's and 1950's by Granholm (1949), Newmark et al. (1951) and Pleshkov (1952). More recent attempts to obtain an exact analysis by Girhammar et al (1991). Girhammar used a beam-column as the subject and adopted an approach that considered the value of slip between the sub elements (K) to be between zero and infinity and to be distributed equally along the length of the beam. Girhammar's analysis developed previous studies by adding second order effects to the formulation and obtained improved prediction of the actual deflections.

Nie and Cai (2003) developed the theory further and were able to produce verified deflection predictions for beams of various loadings using mathematical formulations considering slip factors and partial composite action. Significantly the formulations were also developed for continuous beams but were still limited to two materials and one interface.

In early 2006 a paper was published by Schnabl et.al that developed the continuous beam theory further with the addition of multiple layers and therefore multiple slip surfaces. This formulation was developed to allow use with layers of different thickness and different material types, each with a different slip modulus between layers. This model is very close

to the situation that is the subject of this study however still restricted by assumptions that limit the accuracy of application. The assumptions are common to most previous formulations and are as follows:-

- Materials are linear elastic
- Displacements, strains and rotations are small
- Shear deformations are ignored
- Strains vary linearly over each layer
- The layers are continuously connected and the slip modulus of the connection is constant

These assumptions limit the direct application of Schnabl's formulation to the hybrid arrangement under study for the following reasons:-

- Concrete is a non-linear elastic material.
- Displacements and strains are only small in early stages of loading.
- Shear deformations will affect results due to a span to depth ratio of less than 10.
- Materials not continuously connected but connected by bolts at regular spacing.

These difficulties can be overcome to some extent by the use of finite element method modelling, and in 2006 Al-Amery and Al-Mahaida published the a paper on the numerical analysis of multilayered beams with partial interaction which matches closely the situation in this study and introduces the numerical model as a means of resolving the difficulties.

Numerical analysis literature review

Increasing capacity and speed of computers and better general access to numerical analysis programs have increased the amount of research carried out in the area of modelling the materials and interactions that are pertinent to this study. Areas to review are; modelling of the materials themselves, modelling of the material interactions such as FRP connections and shear connectors, modelling composite members with partial interaction and the choice of modelling program.

In 1998 Barbosa et al reviewed the difficulties of modelling concrete behaviour in a computer program and studied a single span reinforced concrete beam using ANSYS. Eight different concrete models were reviewed and compared, each of these models was valid within ANSYS but difficulty in adequately modelling crushing of concrete and yielding of steel meant that prediction of ultimate loads were not reliably obtained by the program. It was also determined that non-linear stress-strain relations for concrete were essential for any reasonable prediction of deflection.

Fanning (2001) studied numerical models of concrete beams using the ANSYS program. The study confirmed that concrete modelling is particularly sensitive to the elastic modulus assigned to the concrete and that modelling of the beam beyond the first crack required a non-linear analysis. It also indicated that the model behaved linearly up to the first concrete crack. Fanning reviewed methods of achieving good estimates of the actual elastic modulus of concrete and was satisfied that the guidance given in British Standard 8110 provided a suitable value.

An extensive amount of the research in the field of finite element modelling of composite structures with concrete and FRP was accumulated in the report "Finite Element Modelling of Reinforced Concrete Structures Strengthened with FRP Laminates" prepared in 2001 for the Oregon Department of Transport and the US Federal Highway Administration. This research used ANSYS 1998 as a basis and directed modelling variables to the extent that reinforced concrete element type SOLID65 was recommended for concrete models and type SOLID46 suggested for FRP models to enable modelling of multiple layers of fibre.

Numerical studies of the composite action of beams had been mostly based on two-dimensional analytical models however Queiroz et al (2006) completed a three dimensional finite element model using the ANSYS program. Quiroz also adopted SOLID65 element type for concrete. In modelling the connection between the two sub elements forming the composite beam a shear connector model of a simple spring was used. This element type is defined as COMBIN39 in ANSYS and the paper concluded that this adequately modelled the shear connections. Quiroz also noted that numerical analysis of the composite beam was not a straightforward process.

Finite element modelling of concrete slabs with FRP bars has been undertaken by El-Ragaby et al (2005) . This study modelled three actual girder bridges in North America with span depth ratios of less than 15 and reported successfully predicting beam behaviour at low load levels.

Finite element modelling of reinforced concrete beams retrofitted with CFRP was used by Pham and Al-Mahaidi (2005) to study in detail the complications regarding de bonding of the CFRP from the concrete. The model used non-linear finite element method and produced a parametric study of the effects of varying amounts of carbon fibre placed on the underside of the concrete beams. The study concluded that an optimum amount of CFRP could be determined by such an analysis.

A number of alternatives are available with regard to methods and programs for numerical modelling of concrete composite beams. Ranzi et al (2006) compared 4 of these methods for modelling a concrete slab and steel I-section composite beam with partial interaction. The methods reviewed were; finite element method, finite difference method, the direct stiffness method and the exact analytical method. The study determined that a finite element method of analysis provided results compatible with the other 3 approaches and that accuracy depended somewhat on the coarseness of the mesh, a finer mesh with a minimum of 8 discretisation points provided suitable accuracy.

CHAPTER THREE: EXPERIMENTAL PROGRAM

CHAPTER THREE: EXPERIMENTAL PROGRAM

3.1 Introduction

This chapter deals with the experimental work carried out in order to study the effect of the hybrid composite action of carbon and glass FRP with concrete in flexure. In addition the experimental study is also to provide a baseline for validation of the results of the numerical model developed to simulate these hybrid composite effects.

The experimental program consisted of preparation and testing to destruction of 3 T-shaped beams of different material arrangements but all of similar proportions. Each beam was tested in flexure and measurements of deflection, strains and load were obtained in order to allow direct comparison between test beams and for comparison with the finite element model output.

Arrangement of the beams in terms of span, material arrangement and width adopted the same details as those used by Biddah (2003). This provided the potential for further independent verification of the results of this study.

3.2 Test Specimens and Setup

This research will study the effects of the combination of GFRP, CFRP and concrete in composite action. In this experimental investigation three levels of composite action were investigated. The arrangements to be tested are as shown in Figure 3.1

The first and lowest level is a GFRP beam with a concrete slab connected at the top. Anchorage to the slab is accomplished by steel shear connectors. This test arrangement

matches the work carried out by Biddah and can be used for calibration of the results of this paper with previous experimental work. This beam is called GFRP (Figure 3.1a) for identification purposes throughout the study.

Levels two and three progressively increase the level of hybrid in the arrangement. Each are GFRP beams underneath concrete as in level 1, with the addition of carbon fibre strips on the underside (tension side) of the GFRP beam. Shear connection of the GFRP to the slab is also provided by steel shear connectors. The CFRP strips were adhesively bonded to the GFRP beam. Two levels of carbon fibre are used; One 80mm x 1.2mm strip with Beam CFRP1 shown in Figure 3.1b.and two 80mm x 1.2mm strips with Beam CFRP2 shown in Figure 3.1c

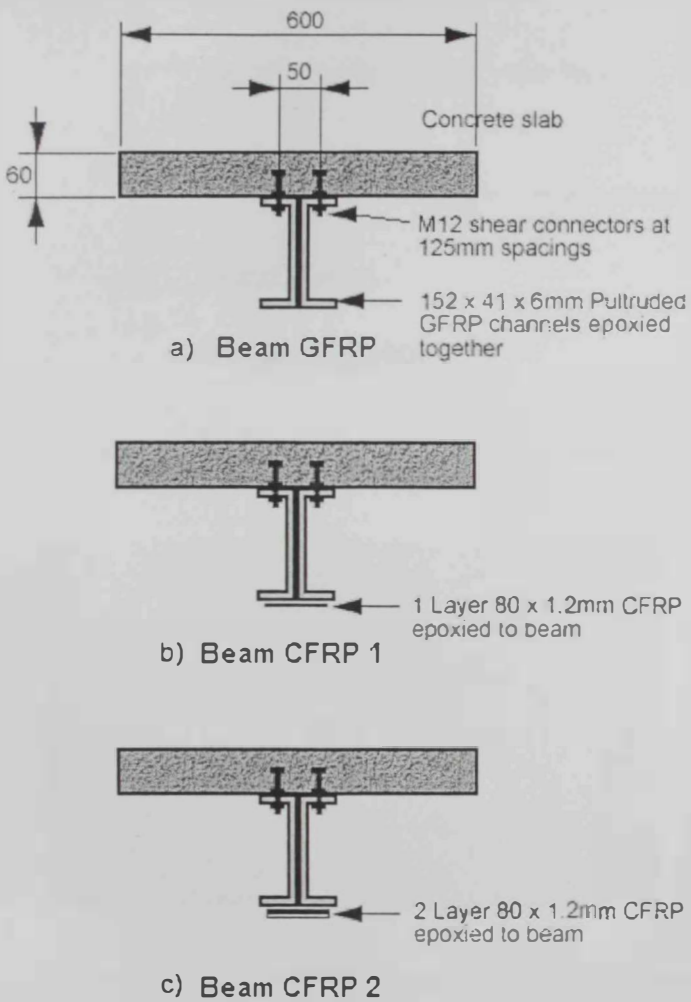

Fig 3.1 *Beam cross sections showing arrangement of test beams*

Details of Test Specimens

Three beam specimens were manufactured and tested to destruction. The arrangement of each specimen is described in detail.

In all cases the GFRP section was fabricated from two back to back pultruded channels of size 152mm x 42mm with 6mm thick web and flanges (Figs 3.2 and 3.3). These were bonded together with a two component epoxy resin based adhesive supplied by Degussa Construction Chemicals.

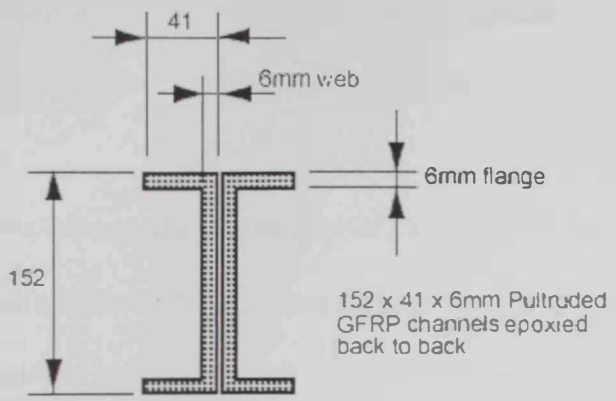

GFRP Arrangement

Fig 3.2 *Cross sectional detail of GFRP beam for all test beams*

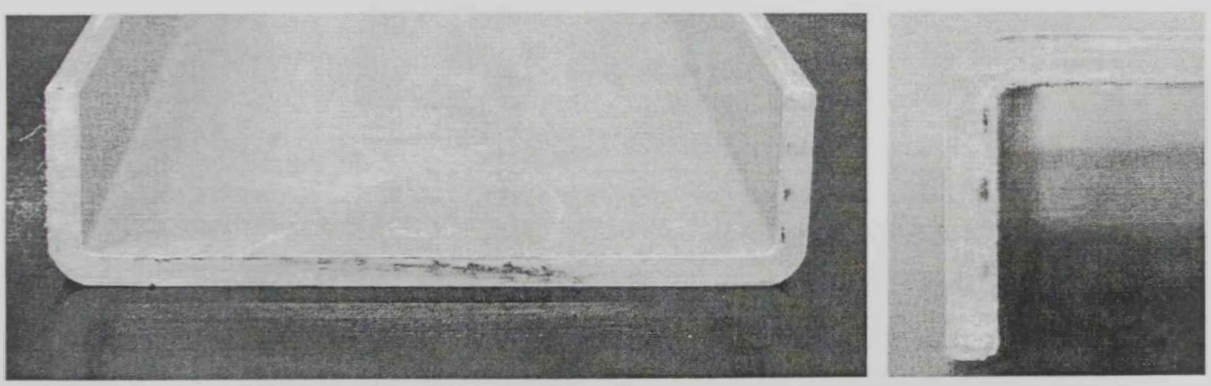

Fig 3 3 *Image of single pultruded Extren GFRP channel showing cross section and corner detail*

Beam GFRP

Test Specimen GFRP consisted of a concrete slab connected to the top of the GFRP beam (Figure 3.1a). The specimen includes the following features:

- GFRP has a full length of 2.25m with 100mm support overhang giving it a span of 2.05m.
- The concrete slab is 600mm wide and 60mm thick, cast directly against the top surface of the GFRP beam.
- Minimal reinforcement of four 10mm bars in the longitudinal direction and 10mm bars at nominal 200mm centres in the short direction are placed in the slab at mid concrete depth
- Shear connection between the slab and the GFRP beam was provided by two rows of 12mm bolts at a uniform longitudinal spacing of 125mm. The cross gauge of the bolts was 50mm. The height of the bolt above the slab to GFRP beam interface was 40mm.
- GFRP stiffeners were glued into place both sides of the flange at the support points and the load points.

Beam CFRP1

Test Specimen CFRP1 consists of a concrete slab over the GFRP beam with the addition of one strip of CFRP underneath the beam (Figure 3.1b and Figure 3.4). The specimen includes the following features:

- CFRP1 was 2.25m in length with 100mm support overhang giving it a span of 2.05m.

- Details of the slab, GFRP beam and shear connectors are the same as for GFRP
- 6mm thick GFRP stiffeners were epoxy bonded to both sides of the beam at 125mm centres. Fly braces were added at the extreme ends of the beam to prevent web failure at the supports
- The back to back channels were bolted together at the ends to ensure that de-bonding and separation of the two channels do not occur.
- One 80mm x 1.2mm CFRP strip was epoxy bonded to the underside of the full 2.25m length of the GFRP beam.

Beam CFRP2

Test Specimen CFRP2 consists of a concrete slab over the GFRP beam with the addition of two strips of CFRP underneath the beam (Figure 3.1c and Figure 3.4). The specimen includes the following features:

- CFRP2 was 2.25m in length with 100mm support overhang giving it a span of 2.05m.
- Details of the slab, GFRP beam, shear connectors, stiffeners and fly braces are the same as for CFRP1
- Two 80mm x 1.2mm CFRP strip were epoxy bonded to the underside of the GFRP beam. The strips were epoxy bonded one on top of the other as the narrow width of the beam did not allow side by side placement.

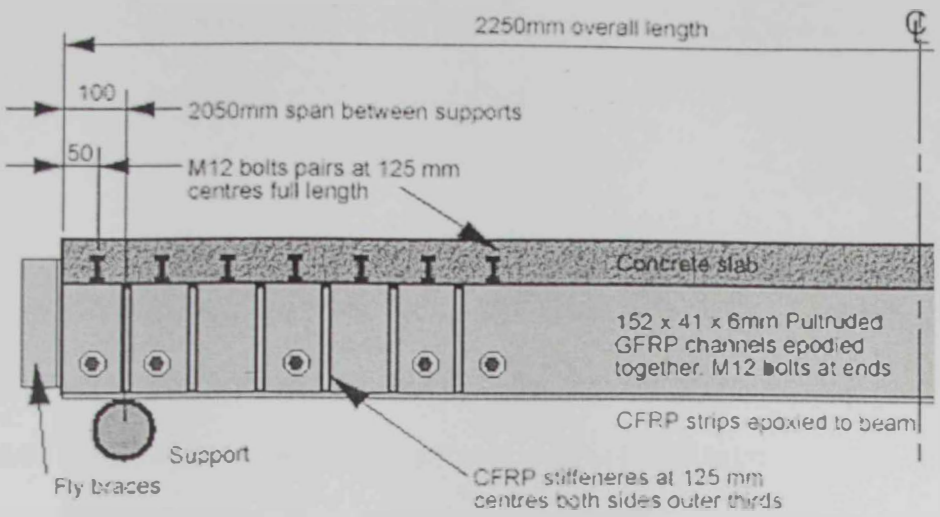

Fig 3.4 *Half elevation of beams CFRP 1 and CFRP2 showing stiffeners and fly braces*

Fabrication of Test Specimens

Fabrication of the three test specimens was simplified by one of the main advantages of fibre reinforced plastic material. The light weight of these materials made handling and preparation a lot easier than if steel was the main beam material.

First the pultruded GFRP sections from Extren were cut to length and the top surface was drilled in preparation for the shear connectors. The holes were 11mm diameter which provided a tight fit for the M12 bolts used as shear connectors. The holes were drilled at 125 mm spacing along the beam. Pairs of GFRP beams were then epoxy bonded together, the epoxy was applied over the entire contact area of the sections.

Shear connector bolts were secured in the holes along the top face of the beam. The bolts were M12 x 50 and were fixed so that the head would be embedded 40mm into the concrete slab, leaving 20mm cover above the bolt.

Strain gauges were fitted, to the bottom edge of the GFRP. Then one layer of CFRP was bonded to the underside of the GFRP beams. The width of the CFRP strip was 80mm and the width of the two beam flanges was 82mm therefore the epoxy contact area was essentially the full width of both the CFRP strip and the GFRP beam.

The beam designated as CFRP2 received a second strip of CFRP. This was the same dimension as the first and was epoxied on the underside of the first strip.

Two strain gauges were fitted and glued to the mid-width point of the top flange surface of the GFRP beams at mid span and the 3 beams were fitted into pre-prepared concrete forms, the reinforcing was placed at mid slab depth and concrete was poured, vibrated and levelled. Test cubes for crushing at 28 days were prepared at this stage. To assist curing the concrete was covered with plastic for 7 days

After the beams were removed from the forms the stiffeners and fly braces were added using epoxy adhesive and strain gauges were added to the top surface of concrete and the underside of the CFRP. Figure 3.5 shows stages of the preciously described steps.

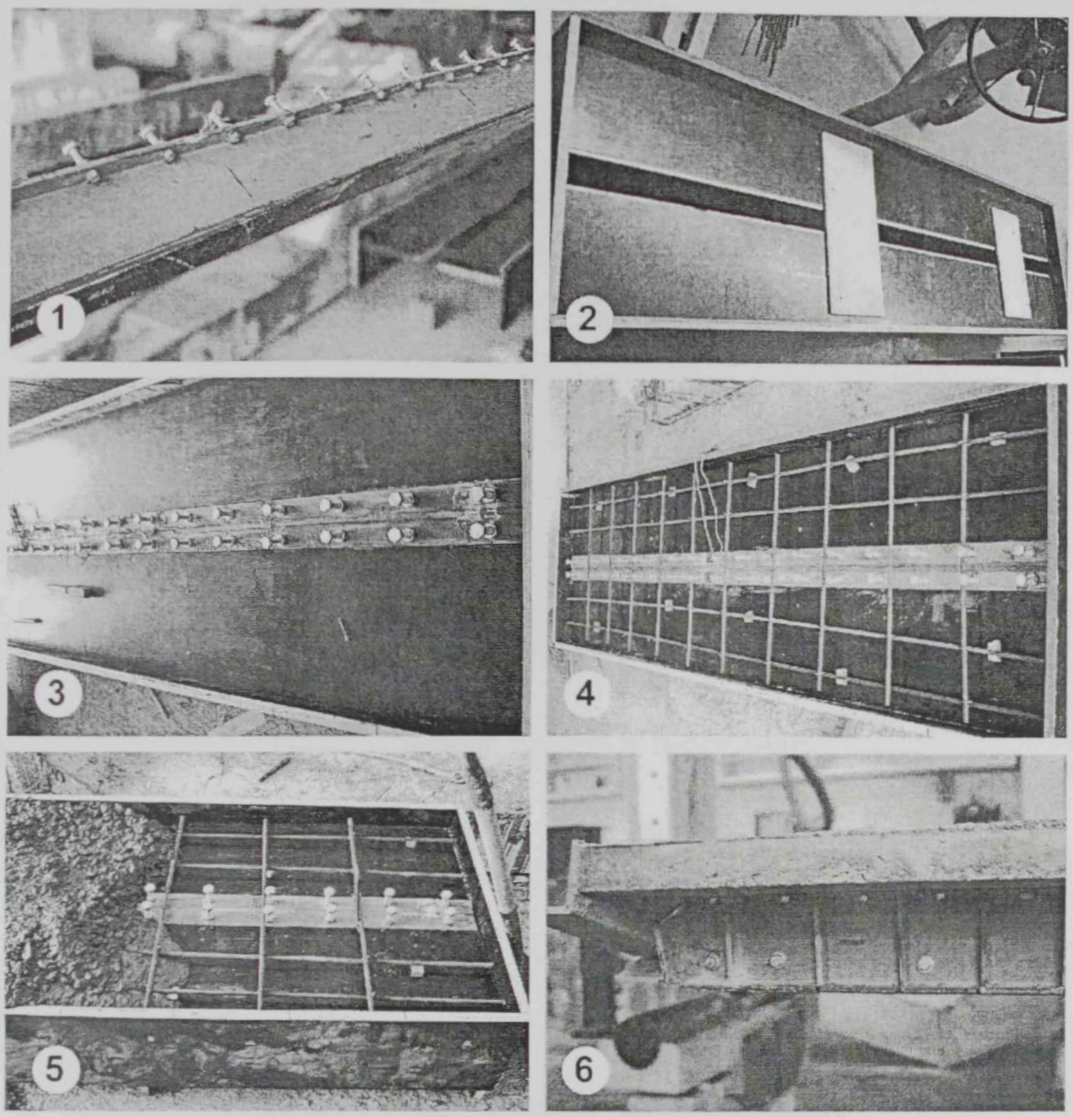

Fig 3.5 *Test beam fabrication: 1. GFRP, CFRP and shear connectors, 2. Formwork ready to receive beams, 3. Beams with strain gauges placed in forms, 4. Reinforcing in place and beams ready for concrete topping, 5. Pouring concrete into formwork with beam, connectors and strain gauges all in position, 6. Finished beam with stiffeners, bolts and fly braces in place.*

Testing Arrangement

Testing was carried out in a test frame capable of up to 200kN. Loading and supporting arrangement for beam GFRP applied 4 point bending over a simply supported span of 2.05 metres. Loads were applied at third points which were 683mm from each support.

Loading was incremental and was applied in approximately 3kN increments. Loading was continued up to failure of the specimen.

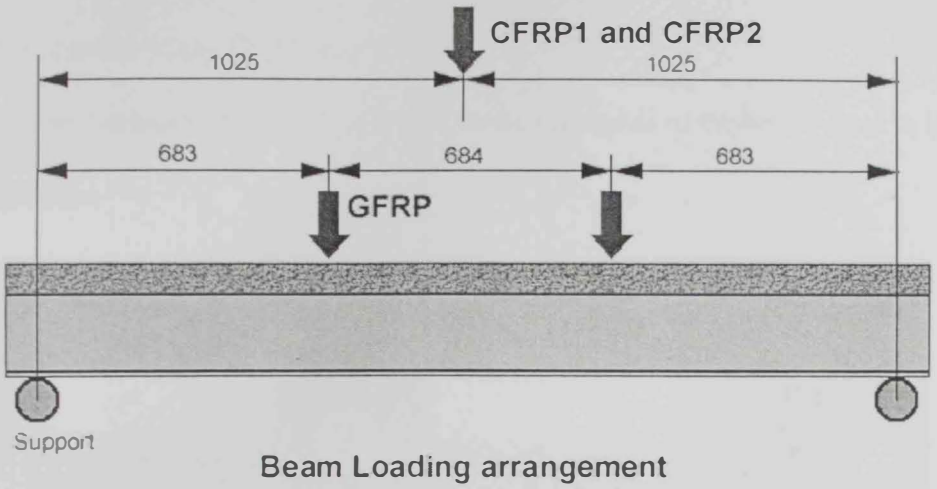

Fig 3.6 *Loading and support arrangement for all beams*

Loading and support arrangements for CFRP1 and CFRP2 were such to provide 3 point bending over a simply supported span of 2.05 metres, the loads were applied at the mid span position. This change of load arrangement was necessary to achieve specimen failure within the capacity of the test frame.

Loading was incrementally applied in approximately 2-5kN increments. Loading was continued up to failure of the specimen.

In all test beams except beam GFRP electrical strain gauges were placed at mid span in the

following positions.

- Beam GFRP: Top of GFRP beam which is the concrete/GFRP interface, and underside of the beam which is the under surface of the GFRP. The strain gauge at top of concrete was placed 150mm off the beam centreline to allow for the mid span load application
- Beams CFRP1 and CFRP2: Top of concrete, top of GFRP beam, underside of beam which is the GFRP/CFRP interface, mid depth of GFRP section and underside of the CFRP strip

Deflections were measured by means of LVDT at the underside of the beam, again at the mid span position.

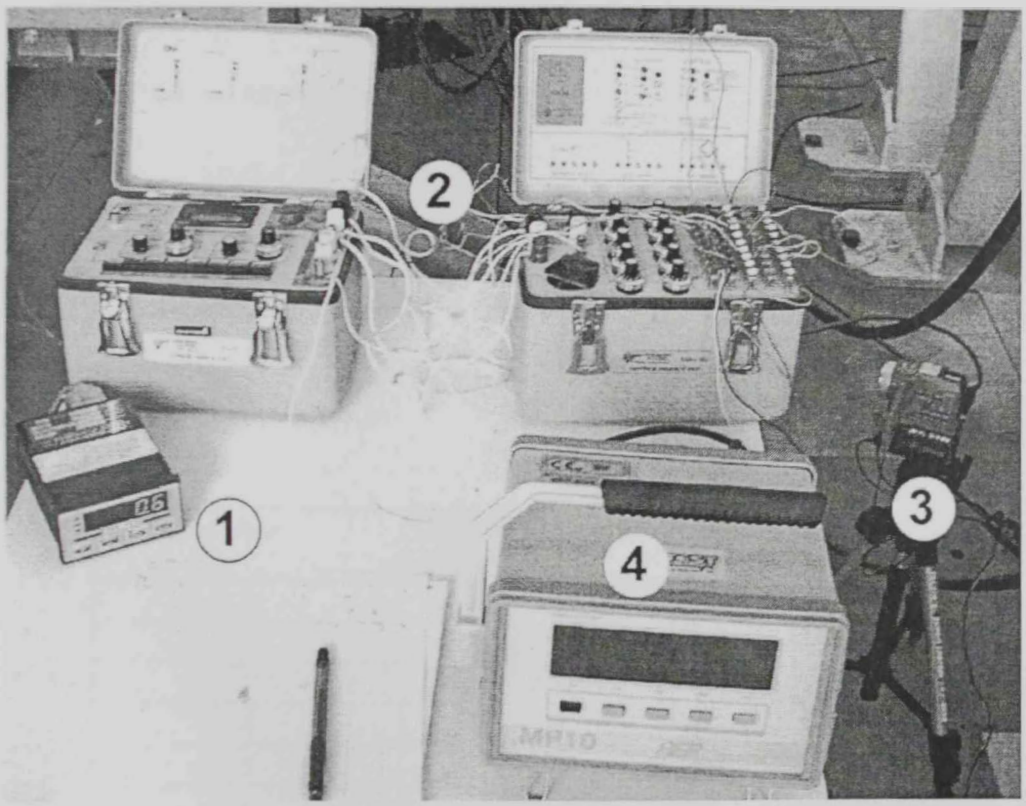

Fig 3.7 *Data recording arrangement during testing: 1. deflection, 2. Strain data recorders, 3. Video camera, 4. Load recorder*

3.3 Material and Section Properties

Concrete

Concrete forms the dominant material in the section. To ensure the properties such as compressive strength and elastic modulus were as consistent as possible the same concrete mix was used for each beam and they were all poured on the same day. The concrete mix used for the slabs was as follows:-

- 50 kg cement
- 32.5 kg water
- 130 kg sand
- 83 kg large aggregate (19mm)
- 35 kg medium aggregate (9.5mm)

For determination of concrete compressive strength 6 concrete cubes were taken on the day of pouring and crushed 28 days later. A summary of the concrete compression test results is as follows in Table 3.1.

Cube Number	28 day compressive strength (MPa)
1	41.0
2	38.3
3	41.0
4	35
5	36.5
6	38.3
Average	38.3

Table 3.1 Concrete compressive strength test results and average

Pultruded GFRP Sections

Pultruded sections were fabricated by EXTREN in Belgium. The section used is a stock channel of catalogue dimensions 6" x 1⅝" x ¼". Actual measured dimensions were as shown in Fig 3.2 . Mechanical and Physical properties of the structural shapes as provided by the manufacturer and adopted by Biddah are given in Table 3.2

Property type	Property	Value
Mechanical Properties	Tensile and compressive strength (MPa)	207
	Shear strength (MPa)	31
	Flexural strength (MPa)	207
	Tensile and compressive modulus (MPa)	17,200
	Full section modulus of elasticity (MPa)	17,200
	Poisson's Ratio	0.33
	Density(g/mm^3)	0.002
Physical Properties	Coefficient of thermal expansion (mm/mm/°C)	$8x10^{-6}$

Table 3.2 Glass fibre reinforced plastic beam material properties

CFRP Strips

CFRP strips were Degussa proprietary MBrace Laminates type CFK 150/2000 supplied in 80mm wide by 1.2mm thick strips. Mechanical and Physical Properties of the material as provided by the manufacturer are given in Table 3.3

Property type	Property	Value
Mechanical Properties	Tensile strength (MPa)	2,500
	Tensile modulus (MPa)	150,000
	Poisson's Ratio	0.3
Physical Properties	Coefficient of thermal expansion (mm/mm/°C)	$8x10^{-6}$

Table 3.3 Carbon fibre reinforced plastic strip material properties

Epoxy Adhesive

The adhesive used to secure the CFRP strips in position was Degussa MBT-MBrace Laminate Adhesives, a two component epoxy resin based adhesive. Mechanical and Physical Properties of the material is given in table 3.4

Property type	Property	Value
Mechanical Properties	Compressive strength (MPa)	>60
	Flexural strength (MPa)	>30
	Modulus of elasticity (MPa)	8500
	Poisson's Ratio	0.3
Physical Properties	Density(g/mm^3)	0.0018

Table 3.4 Epoxy adhesive material properties

Shear Connectors

Shear connectors were galvanized M12 steel bolts of grade 8.8 with 50mm thread length. These bolts were installed with the head approximately 40mm into the concrete. Two nuts were used to secure the bolt to the GFRP.

Shear connectors were installed at 125mm longitudinal spacing's and 50mm cross gauge. (refer to Fig 3.8)

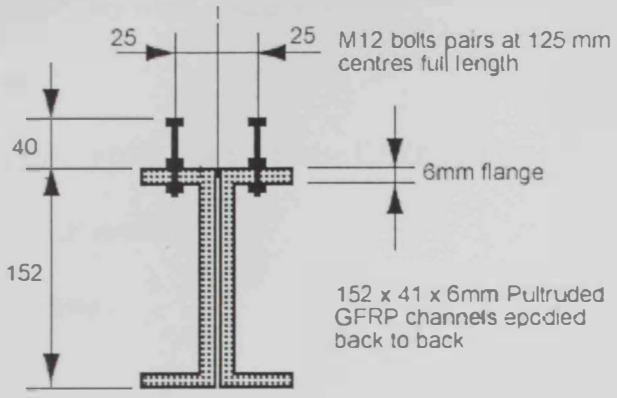

Bolt Arrangement

Fig 3.8 *Shear connector bolts arrangement details*

Strain Gauges

The strain gauges were attached to the substrate materials with Locktite manufactured Super-Glue. Strain gauges were Tokyo Sokki Kenkyujo manufactured type FLA-5 11-3L with a 5mm gauge length.

Strain gauge positions (Fig 3.9) on Beam GFRP were at mid span except for the top of concrete strain gauge. They were placed at levels:-

- Top of concrete. This strain gauge was 150mm off the mid span to allow for mid span load application.
- Top of GFRP beam which is the concrete/GFRP interface
- Underside of the beam

Strain gauges on Beams CFRP1 and CFRP2 were at mid span except the top of concrete gauge which was placed 150mm off the centre point to allow loading of the beam at mid span for 3 point bending. They were placed at levels:-

- Top of concrete
- Top of GFRP beam which is the concrete/GFRP interface
- Mid depth of GFRP section
- Underside of the beam

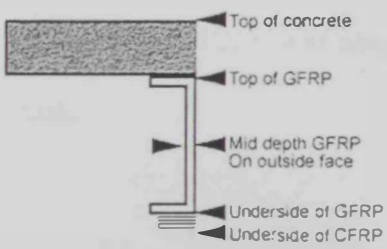

Strain Gauge Arrangement

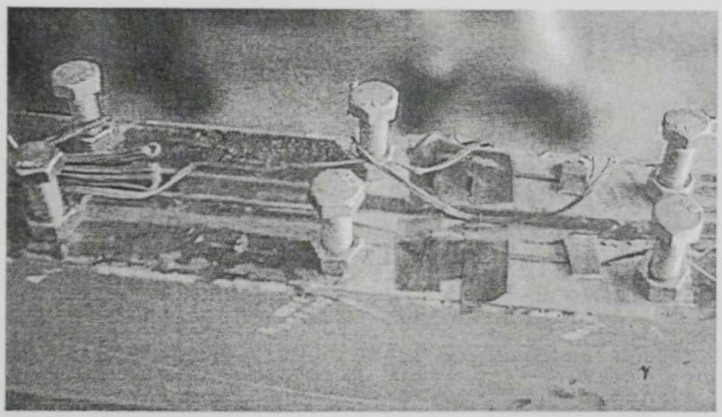

Fig 3.9 *Shear Strain gauge location and image of top of GFRP gauges in position*

3.4 Test Results and Discussion

Testing of the 3 specimens Beam GFRP to Beam CFRP2 was carried out in the 200kN test frame. Test specimens were loaded incrementally through to failure and details of the beam behaviour were recorded by:

- Strain gauges placed at mid span measured strain levels
- A LVDT at mid span measured mid span deflection
- Photographic and video recordings

Load levels were read from the test frame hydraulic controls

Behaviour of the test beams

Calibration Beam GFRP

Test specimen beam GFRP was the first beam tested. Beam response to loading was recorded to form a baseline for comparison of the effects of CFRP addition in beams CFRP1 and CFRP2. It was also available to assist in referencing previous work by A. Biddah.

Beam GFRP was tested under 4 point bending (Fig 3.10-1). The load was applied through a spreader beam in increments of approximately 2.5kN and continued up to beam failure. Application of the load at the third points was through a spreader rod that ensured that the load was applied equally across the full width of the beam.

The beam failed at a load level that was close to the loading jack maximum and some difficulty in applying a load increase smoothly was encountered. Two times the load was released slightly to stop juddering at around 160kN. When the juddering was under control the load was reapplied. This may have affected the results between 160kN and the failure load of 175 kN. Due to this condition the testing arrangement for Beam CFRP1 and Beam CFRP2 was changed to 3 point bending so that beam failure loads would be below the limits of the loading jack.

At a load of 35kN there was a loud bang but inspection of the beam showed no obvious source of the noise. Analysis of the test data suggests that this noise was generated by the breaking of the adhesive bond between the concrete and the top surface of the GFRP.

From approximately 117 kN onwards cracking sounds were audible at every load application. Also at this point small cracks in the transverse direction were observed on the underside of the slab at the left hand load point. (Fig 3.10-4)

Failure was finally by web instability at the left hand end (Fig 3.10-2). The failure was sudden.

Inspection of the beam after failure showed the following features:

- Folding of the web at the left hand end and de-bonding and separation of the webs of the two channels
- Longitudinal crack along the centre-line of the beam
- Crescent shaped concrete cracking emanating from each of the last few shear

connectors at both ends of the beam

- Rotation of shear connectors at each end of the beam, also evidence of local failure of the GFRP around the shear connectors. (Fig 3.10-3)
- No sign of fracture or splitting of the GFRP between the shear connectors along the length of the beam was evident

Ultimate Load in 4-point loading (kN)	Ultimate Moment (kN-m)	Ultimate deflection (mm)	Top strain at failure	Bottom strain at failure	Mode of failure
175 kN	60 kN-m	48.4 mm	-0.00229 (compression)	+0.01174 (tension)	Web instability at support

Table 3.5 Test Result for Beam GFRP

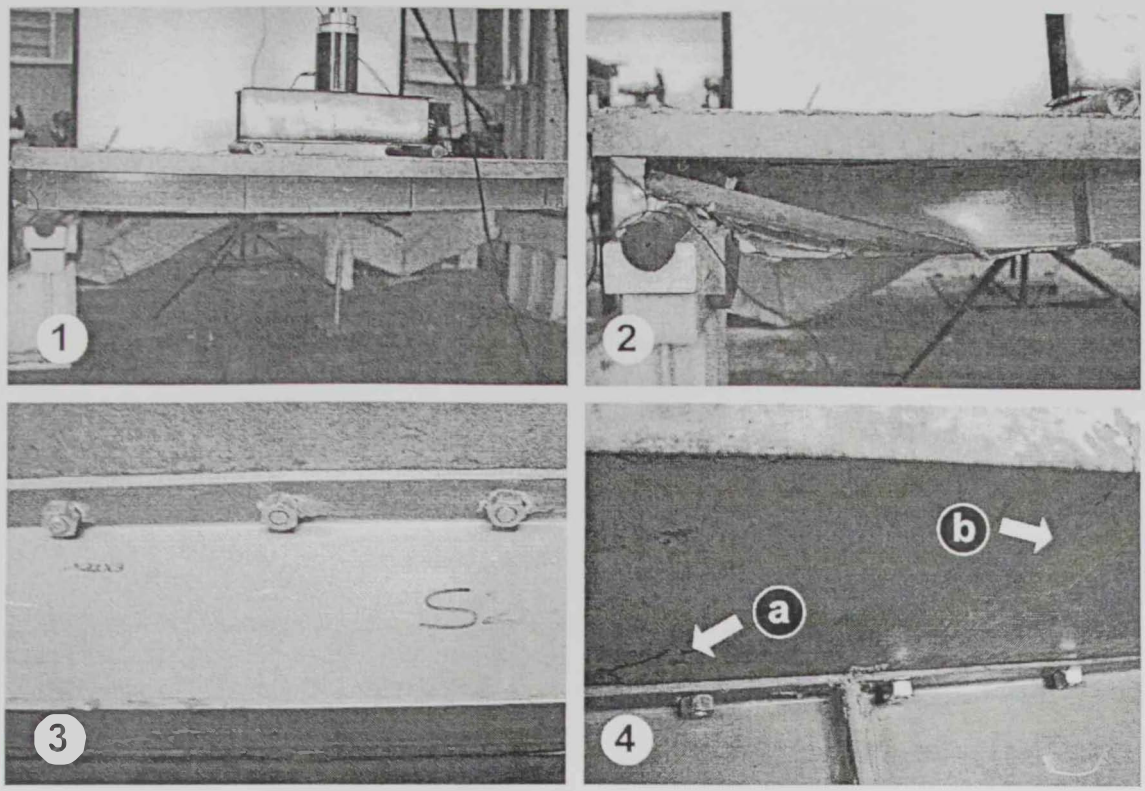

Fig 3.10 *GFRP testing images 1. Test set up with 4 point loading, 2. Web buckling failure of GFRP beam over one support, 3. Deformation of GFRP at shear connectors at beam ends , 4. Cracks in the underside of the slab: a) curved crack around shear connectors on support side b) transverse cracks.*

Hybrid Composite Specimens CFRP1 and CFRP2

The mode of failure in beam GFRP led to modification of the remaining beams in an attempt to force a flexural mode of failure. To do this stiffeners were placed within the webs of the GFRP channels and bolts were installed holding the flanges together to prevent de-bonding and separating as had occurred in beam GFRP. At the ends of the beam fly braces were added between the GFRP beam and the concrete slab, these braces and the web

stiffeners were expected to work together to prevent rotation of the beam ends.

Beams CFRP1 and CFRP2 were placed in the 200kN jacking frame and were subjected to load in 3 point bending. Load was applied at mid span and a spreader rod was used to ensure the load was applied equally across the full width of the beam (Fig 3.11-1). The load was raised in increments of approximately 5kN and continued up to beam failure. The results are shown in Table 3.6

Test Specimen	Ultimate Load in 3-point bending (kN)	Ultimate Moment (kN-m)	Ultimate deflection (mm)	Top strain at failure	Bottom strain at failure	Mode of failure
Beam CFRP1 1 CFRP strip	100	51.25	20.7	-0.00118	+0.00573	De-bonding of CFRP
Beam CFRP2 2 CFRP strips	171	88	40	-0.00172	+0.00807	De-bonding of CFRP

Table 3.6 Test Results for Beam CFRP1 and Beam CFRP2

Beam CFRP1 failed by de-bonding of the CFRP at a load of 100 kN. The CFRP de-bonding at 100kN occurred suddenly with a loud bang. The de-bonding happened over the entire length of the beam. The CFRP remained unbroken over its full length.

Inspection of beam CFRP 1 after failure showed the following features:

- Lateral concrete cracking on the underside of the slab extending the full width of the beam at mid span (Fig 3.11-3)
- CFRP de bonding over full length of the beam
- Crushing of the concrete on the top surface of the beam in the region of the loading rod (Fig 3.11-2)

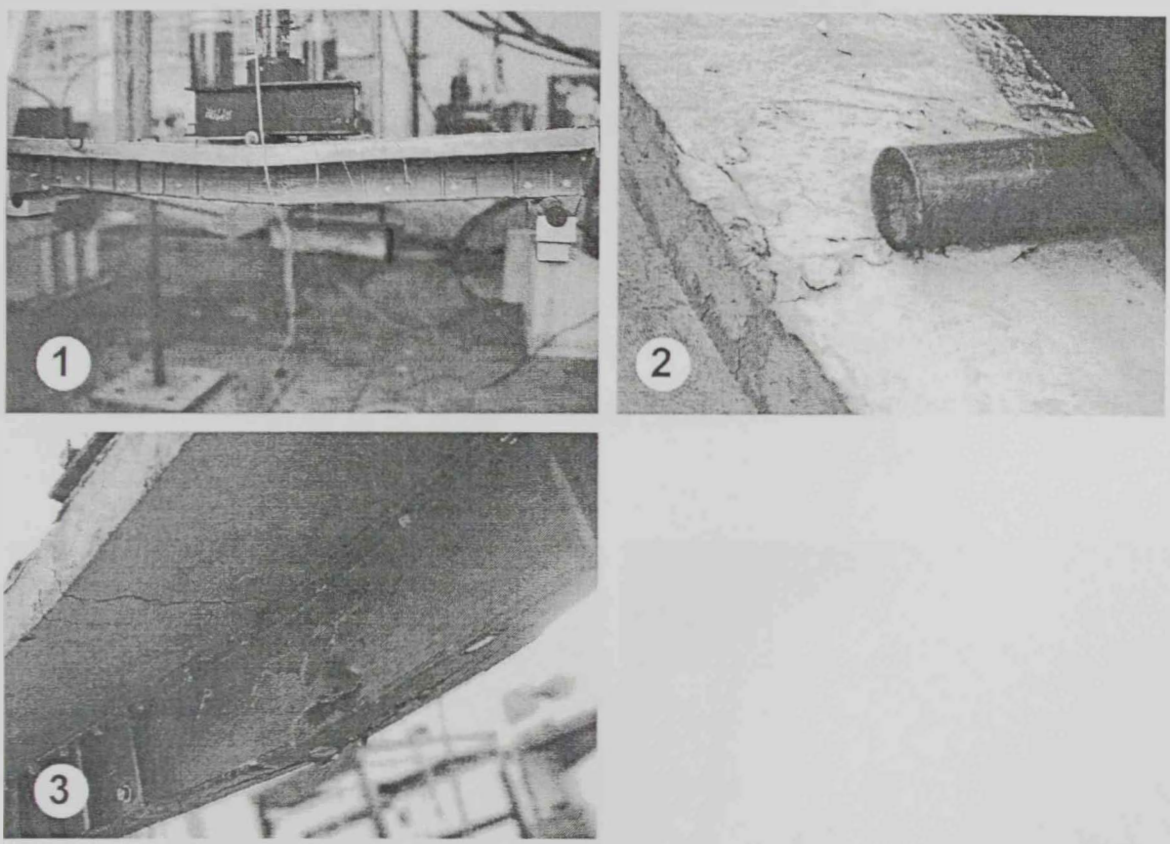

Fig 3.11 *CFRP1 testing images 1. Test set up with 3 point loading, this image is after CFRP bond failure, 2. Concrete crushing on the slab top surface under the mid span loading bar, 3. Results of flexural failure of beam with cracks in the underside of the slab and failed GFRP*

Beam CFRP2 continued to 171 kN before de-bonding of the CFRP. Again the de-bonding was sudden, this time occurring over two thirds of the length of the beam. At the point where the adhesive bond remained intact, about 400mm from the right hand support, the CFRP showed some damage and a few broken fibres but not major failure. After approximately 125 kN crushing of the concrete top surface near the loading rod was also observable, this is confirmed by the strain readings which reached a maximum strain of approximately -0.002 at this load but did not increase when the load was increased beyond this value.

Inspection of beam CFRP2 after failure showed the following features:

- Lateral concrete cracking on the underside of the slab extending the full width of the beam at mid span (Fig 3.12-2)
- CFRP de-bonding over two thirds of the beam length (Fig 3.12-1)
- Slight rotation of shear connectors at the ends of the beam and evidence of local deformation of the GFRP around the shear connectors.

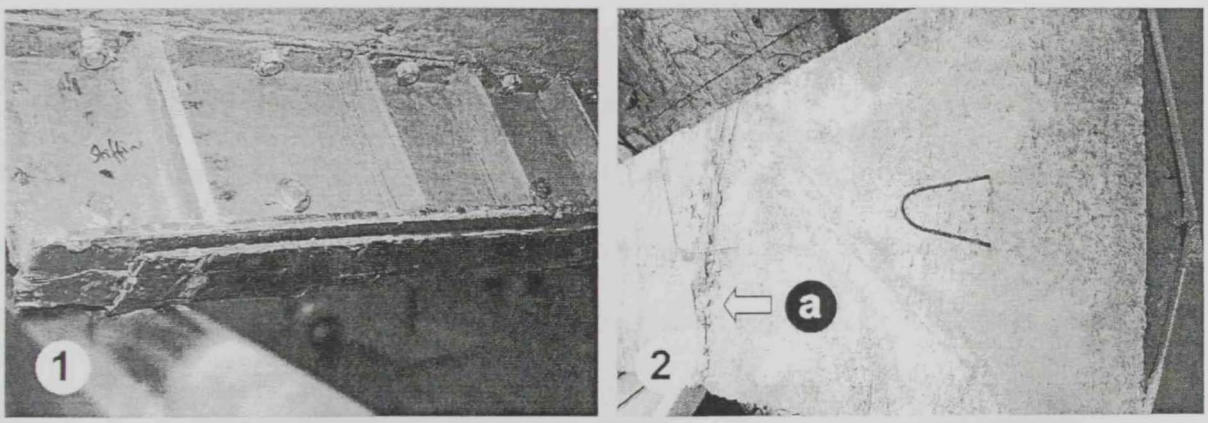

- Crushing of the concrete on the top of the slab in the vicinity of the loading rod.

Fig 3.12 *CFRP2 testing images 1. CFRP delamination at one end, 2. Concrete top surface cracking: a) compression failure full width at mid span*

Load Deflection Behaviour

Deflection was measured by LVDT at mid span of the beams. When the load and deflection values are plotted it clearly shows that the addition of carbon fibre strips reduces the deflection of the beam for a given moment and increases the moment carrying capacity providing the strips remain bonded to the structure.

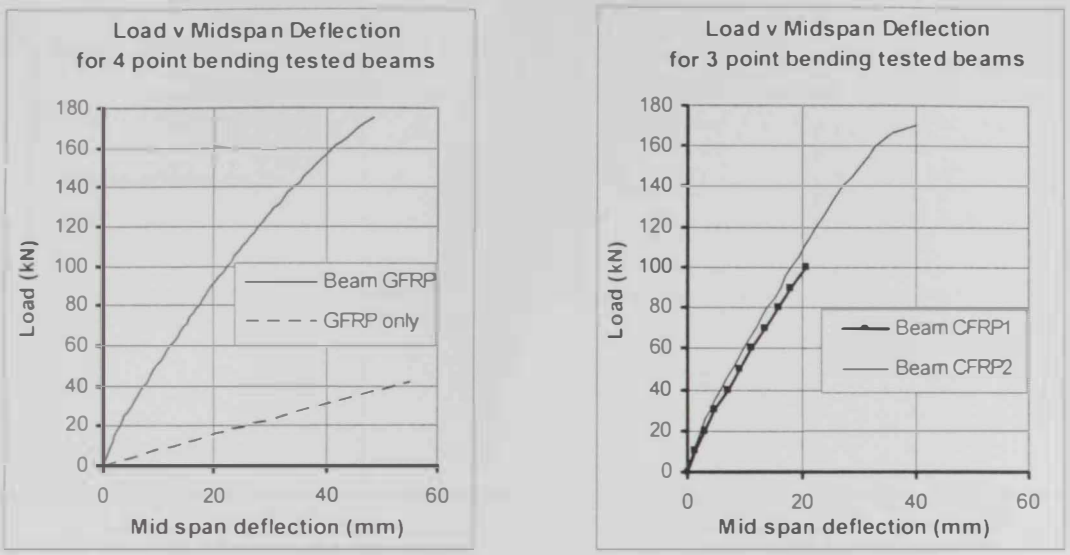

Fig 3.13 *Comparison of load verses mid span deflection for all tested beams and a GFRP only beam*

Fig 3.13 compares load and deflection for all beams and indicates the increased stiffness provided by the addition of a single strip of CFRP (Beam CFRP1). The addition of a second strip as for sample Beam CFRP2 provided a relatively small increase in stiffness. A comparison of ultimate load could not be completed due to the premature de-bonding of carbon fibre from CFRP1. The estimated load deflection curve for a GFRP beam only (without concrete top or CFRP underside) has been calculated and is also shown for comparison. This curve indicates the significant stiffness gain achieved when the concrete slab is added and working in composite with the GFRP beam.

Test Specimen	Ultimate Load (kN)	Ultimate Moment (kN-m)	Ultimate deflection (mm)
GFRP only (calculated)			
3 point bending	42	22	55
4 point bending	63	22	
Beam GFRP: GFRP and concrete slab 4 point bending	175	60	48
Beam CFRP1: 1 CFRP strip on underside 3 point bending	100	51	21
Beam CFRP2: 2 CFRP strips 3 point bending	171	88	40

Table 3.7 Comparison of load and deflection of each beam type considered

Beam response to increased load is close to linear for most of the loading range. Prior to around 10% of failure load the beams displayed higher overall stiffness. This is possibly due to the absence of any slip between GFRP beam and the concrete slab. Between 10% and 80% the graphs are approximately linear with some loss of stiffness evident in the slight curvature. After around 80-90% of failure load is applied the beams become increasingly non-linear with an effective loss of stiffness at higher load levels.

Material Strains

Strain recordings were important in the determination of the effects of the hybrid composites and to provide a baseline for validation of the numerical model.

Longitudinal strain was recorded at or near mid span providing data for the following positions (Fig 3.15):-

- Top of concrete, these gauges were 150mm from mid span in beams Beam CFRP1 and Beam CFRP2
- Interface of concrete and GFRP, these gauges were placed on the GFRP section
- Mid depth of the GFRP
- Underside of the GFRP
- Underside of the CFRP

These strains are shown in Figures 3.16 to 3.18. Compressive strains are shown as negative (-) and tensile strains are shown as positive (+).

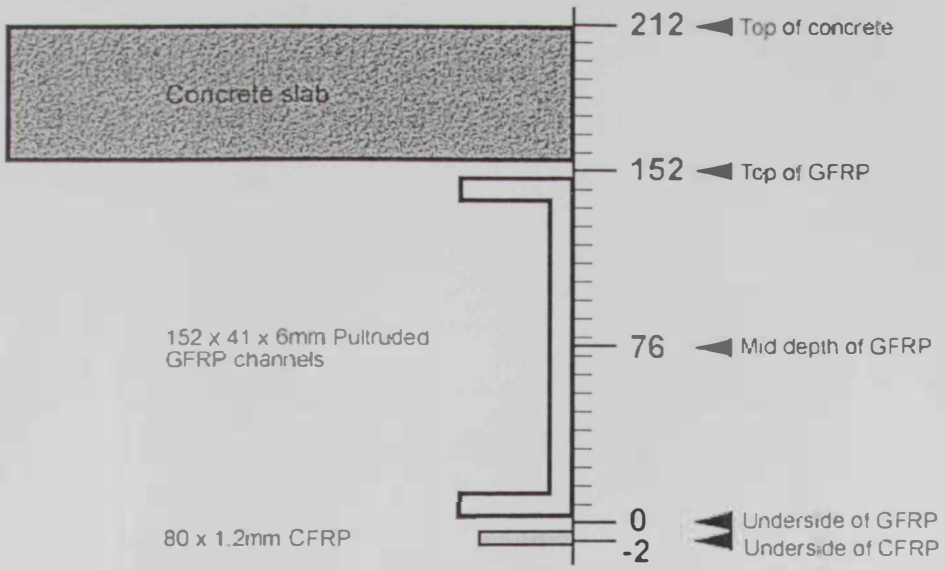

Fig 3.15 *Positions of strain gauges and key to graphical representation of strain in strain verses beam depth graphs that follow.*

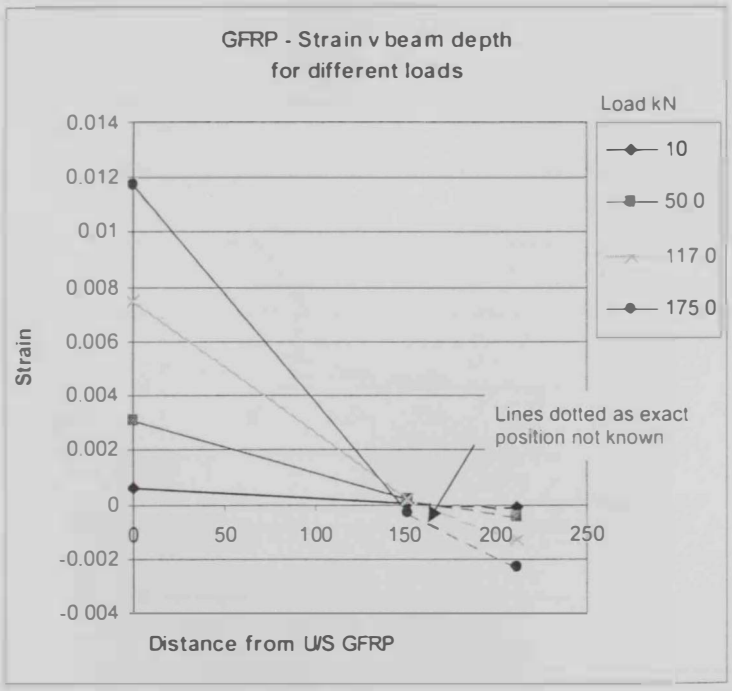

Fig 3.16 *Beam GFRP - Measured strains plotted against beam depth for different loads*

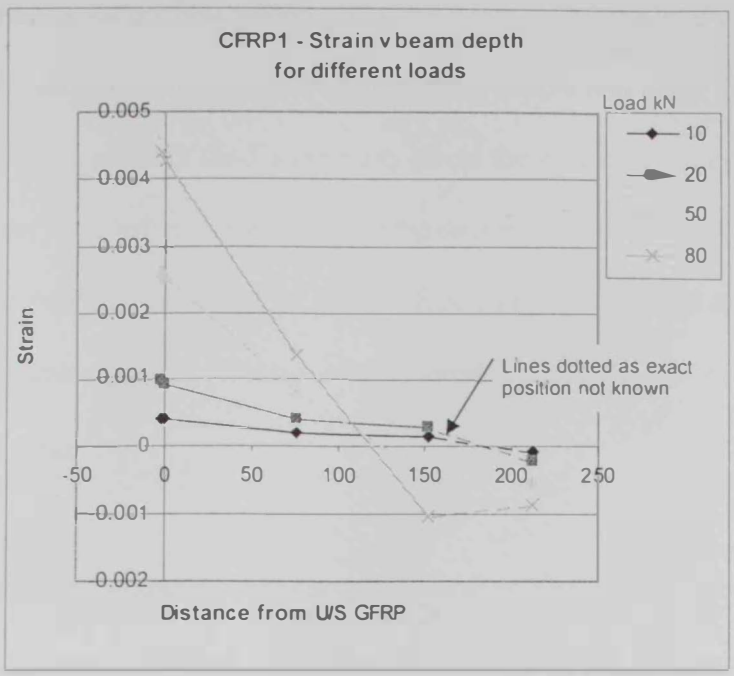

Fig 3.17 *Beam CFRP1 with 1 carbon strip - Measured strains plotted against beam depth for different loads*

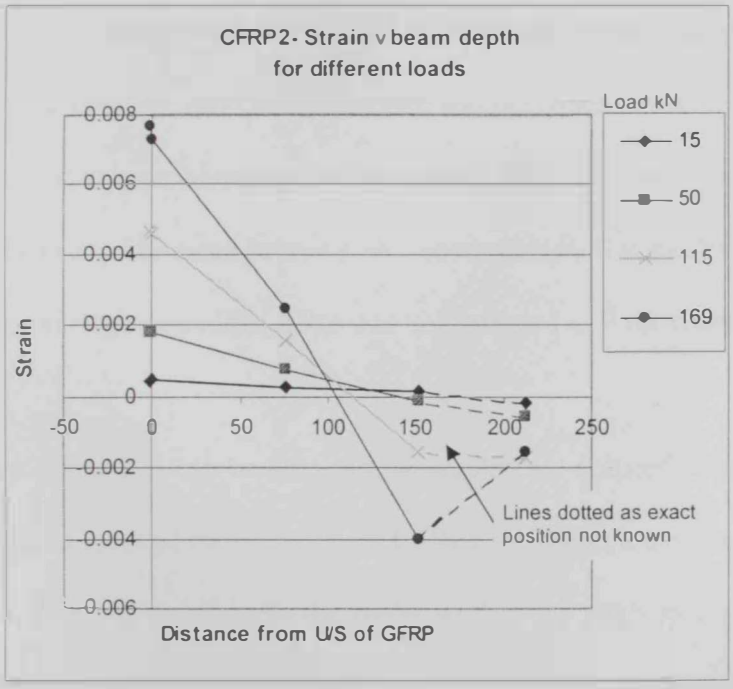

Fig 3.18 *Beam CFRP2 with 2 carbon strips - Measured strains plotted against beam depth for different loads*

Plotting of the strain profiles indicates that for Beam GFRP the neutral axis was initially within the depth of the concrete slab and the strain profile was linear at low loads. As the load increased the effect of the discontinuity across the shear connectors increased. A strain gauge was not installed on the underside of the concrete slab so the strain profile within the depth of the concrete could not be plotted, however the numerical analysis reported in chapter 4 indicates that the underside of the concrete experienced positive strain throughout the loading range.

Observation of the strains recorded at the top of the GFRP shows that while at low loads the change in strain moved in a positive direction indicating increasing tension as load increased. This confirms that the neutral axis is initially within the depth of the concrete. As load increased the strain then began to move in a negative direction. This change from positive to negative change with increasing load represents the load at which the adhesive bond between the concrete and GFRP is broken and full composite action of the section is lost. This occurred at approximately 35kN on Beam GFRP and corresponded to an audible sound from the beam. The same pattern is also observable for Beams CFRP1 and CFRP2 at similar loads, although an audible noise was not recorded in these cases.

For any given moment it can be seen that the strains are reduced from Beam GFRP to Beam CFRP1 and reduced further in Beam CFRP2 showing clearly the advantage of the added carbon strip. As an example the strain profiles for 50kN-m Fig 3.19 shows that GFRP maximum tensile strain reduced from +0.00954 to +0.0038 and compressive concrete strain reduced from to -0.0018 to -0.0014.

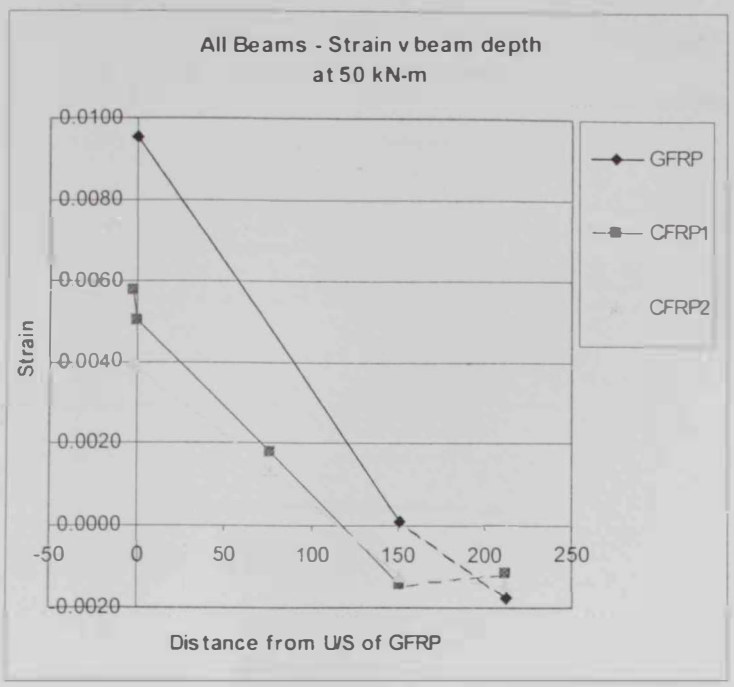

Fig 3.19 *Longitudinal strain plotted against beam depth for all beams at moment of 50 kN-m*

The GFRP strains achieved in Beam GFRP at flexural failure matched closely with manufacturer's data. The failure strain of approximately +0.0117 equates to a stress of 202 MPa, close to the manufacturers guideline of 207 MPa. From this it can be determined that Beam GFRP was close to flexural failure at the time of web failure, therefore the test results can be considered as representing the complete range of flexural capacity.

Considering the strain verses load diagrams for each beam test it can be shown that crushing of the concrete occurred around 60 kN-m where the concrete strains recorded begin to regress and become unreliable

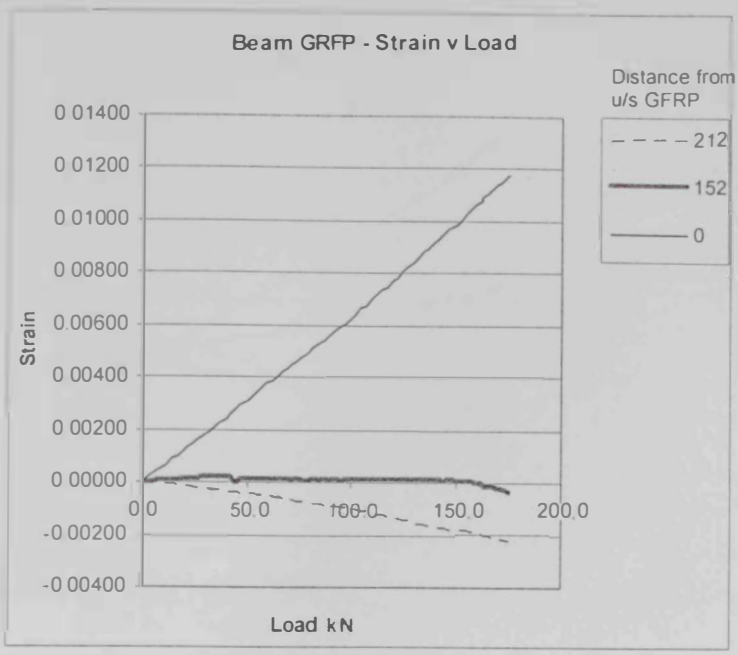

Fig 3.20 *Beam GFRP - Longitudinal strain plotted against load at different beam depth positions*

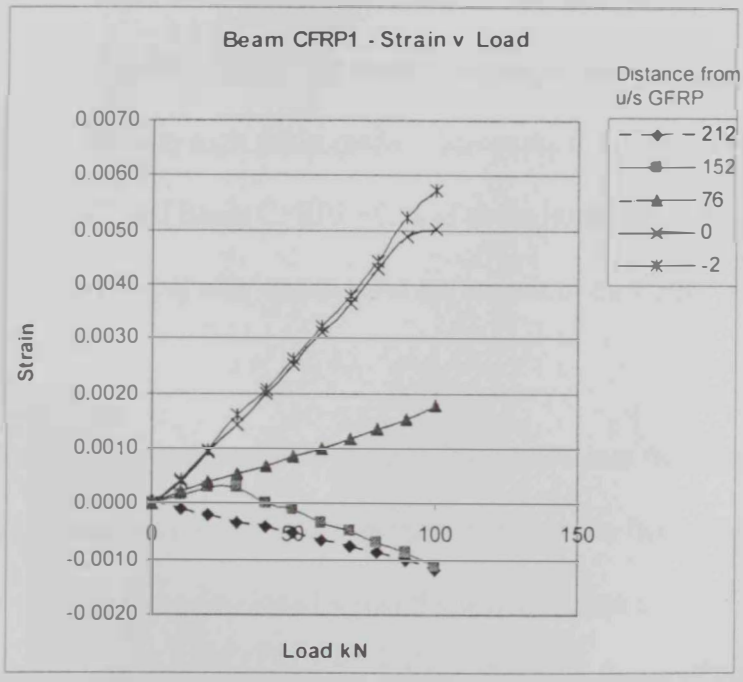

Fig 3.21 *Beam CFRP1 - Longitudinal strain plotted against load at different beam depth positions*

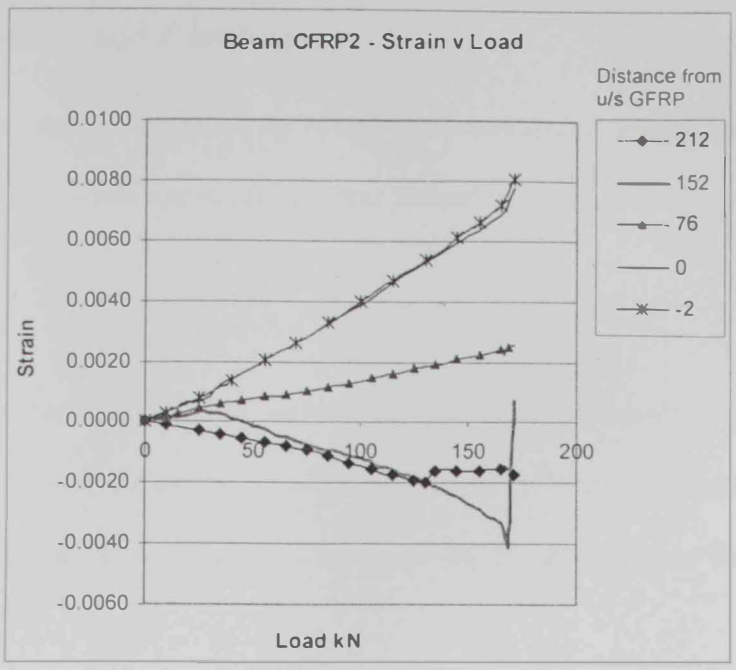

Fig 3.22 *Beam CFRP2 - Longitudinal strain plotted against load at different beam depth positions*

Strain at the underside of GFRP and CFRP follow similar paths however it can be seen that approaching the failure point there is rapid diversion in strain so that immediately before failure there is a very high strain gradient across the thin CFRP strip. In Beam CFRP1 it was +0.0007 and Beam CFRP2 +0.0003 strain immediately before failure. This caused the epoxy to fail after which point the benefit of the CFRP was lost to the section

When these findings are compared with those of Biddah we note that shear connectors spaced at 125mm centres as in this case prevented compression flange buckling and allowed better strength to be developed across the whole section enabling greater load carrying capacity. Close inspection was carried out of the top flange of the GFRP to determine if this closer spacing precipitated splitting of the GFRP. This effect was not observed.

3.5 Summary and Conclusions

In this experimental investigation the hybrid composite system using CFRP, GFRP and a concrete slab has shown a load carrying and deflection control benefit over concrete and GFRP.

It can be noted that the addition of one relatively small carbon fibre strip provided a notable improvement in beam stiffness and load carrying capacity. When a second layer of CFRP is added a similar additional benefit is not achieved, possibly due to limiting adhesive properties.

The use of adhesive to bond the CFRP to the GFRP provides a potential weakness in the hybrid system and an additional difficulty in construction as this is highly sensitive to the quality of workmanship.

Failure by de-bonding of the GFRP was sudden, giving the failure mode a brittle

CHAPTER FOUR: NUMERICAL ANALSYIS AND VALIDATION

CHAPTER FOUR: NUMERICAL ANALSYIS AND VALIDATION

4.1 Introduction

In order that the benefit of the experimental outcomes could be extended beyond the time and materials limitations of physical testing a numerical finite element model was developed to attempt to simulate the beams and their behaviour. This chapter deals with the development and application of the numerical model that may be used to simulate the beam behaviour.

This chapter follows the:-

- Numerical modelling of the problem.
- Description of the finite element (FE) model developed including input parameters for each material.
- Outline of the parametric study used to calibrate the model to the physical tests.
- Results and discussion of the trends identified through the parametric study.
- Comparison of results of the finite element and experimental results.
- Summary and conclusion on the findings identified in this chapter.

4.2 Numerical Modelling of the Problem

The use of the numerical finite element program as a tool for solving complex structural engineering problems is reasonably common as it is capable of modelling many complexities that may exist in a structural system. A numerical model was developed for the beam and material arrangements under study. The model was an attempt to simulate the behaviour of the hybrid composite beam and therefore provide a basis for investigating other future material and arrangement alternatives numerically without the immediate need to test physical specimens. The program selected for this finite element analysis was ANSYS version 10, using the Mechanical Analysis option.

Development of a numerical model for this hybrid composite section is complicated due to the following issues:

- The structural system is composed of 4 different materials, concrete, GFRP, CFRP and epoxy
- The stress- strain relationship of concrete is considerably non-linear above a certain stress level and failure criteria are difficult to define.
- Inter-material interactions between concrete and GFRP through the shear bolts is difficult to accurately model, particularly as failure loads are approached.

- Interaction between GFRP and CFRP via an epoxy adhesive requires the development of a complex bond and failure model.

Model development is limited in this study to the liner portions of the loading curve as

established by the experimental program. This selection of load range is due to the increasing amount of uncertainty that occurs as the beam response to load becomes increasingly non-linear. Provision has been made for future extension of the developed model into the nonlinear regions by the appropriate selection of material types within ANSYS but modelling the beam into non-linear regions and failure is not within the scope of this study. For consistency in comparisons the load selected for numerical analysis is 50kN. This load suits all three experimental beam arrangements and is reached prior to any significant nonlinearity observed in the load – response graphs.

Modelling of the fibre reinforced materials was carried out using two different material type approaches. The CFRP and GFRP elements have material properties that are strong and stiff in the direction of the fibres and weak and less stiff in the other two normal directions. To model this variation in properties orthotropic material properties can be used. Using such properties more accurately represents the fibre reinforced materials in the beams studied. For example the CFRP has a high Elastic modulus of 150,000 N/mm^2 in one direction thanks to the uni directional carbon fibres, however the elastic modulus in the other 2 dimensions is limited to around 3,500 N/mm^2, which is simply the value for the plastic that holds the fibres all together. An alternative material model explored alongside the use of orthotropic properties was using isotropic material properties. An isotropic material has exactly the same properties in all directions. The purpose of using both orthotropic and isotropic properties and running them side by side was to observe the beam behaviour with material changes and to consider weather ignoring the material orthotropy, which is the only option in software other than ANSYS, still provides sufficient accuracy for modelling purposes.

4.3 Description of Finite Element Model

General

The beams modelled are sufficiently simple in form to permit an extrusion approach to build the three dimensional geometric shape. Material properties and Element Types appropriate for ANSYS analysis were selected based on the expected behaviour of the material during linear and non-linear phases of load response. Meshing of the resulting volumes adopted a cubic 3-dimensional arrangement; again this matched the consistency of longitudinal form of the beam. Mesh sizes were adjusted in regions of stress concentrations such as at the beam ends and under the acting loads as shown in Figs 4.1 and 4.2.

One quarter of the beam was created within ANSYS and symmetry boundary conditions were applied at mid span and longitudinally along the centreline of the beam to ensure that a full beam was modelled (Fig 4.3). Loading was applied in 3 point or 4 point bending according to the actual arrangement physically tested.

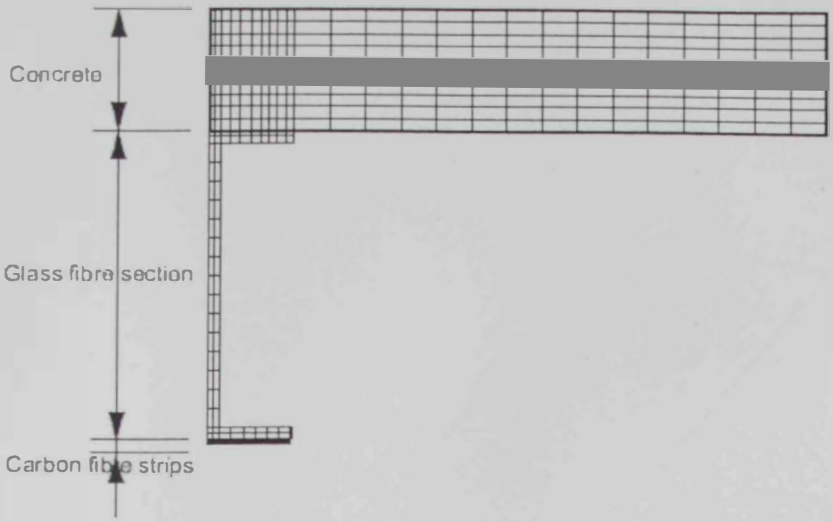

Fig 4.1 Image of rectangular block mesh arrangement on the beam cross section

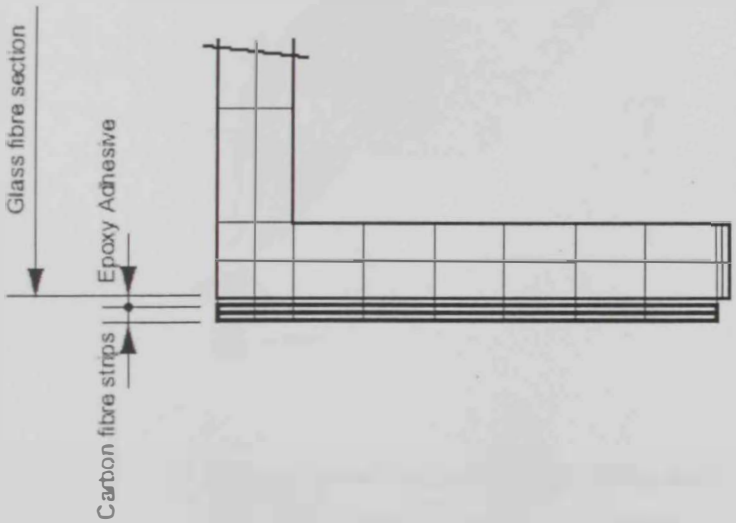

Fig 4.2 Enlarged detail of rectangular block mesh arrangement at the lower GFRP flange and CFRP strips. The two CFRP layers shown here were modelled without a layer of epoxy between them

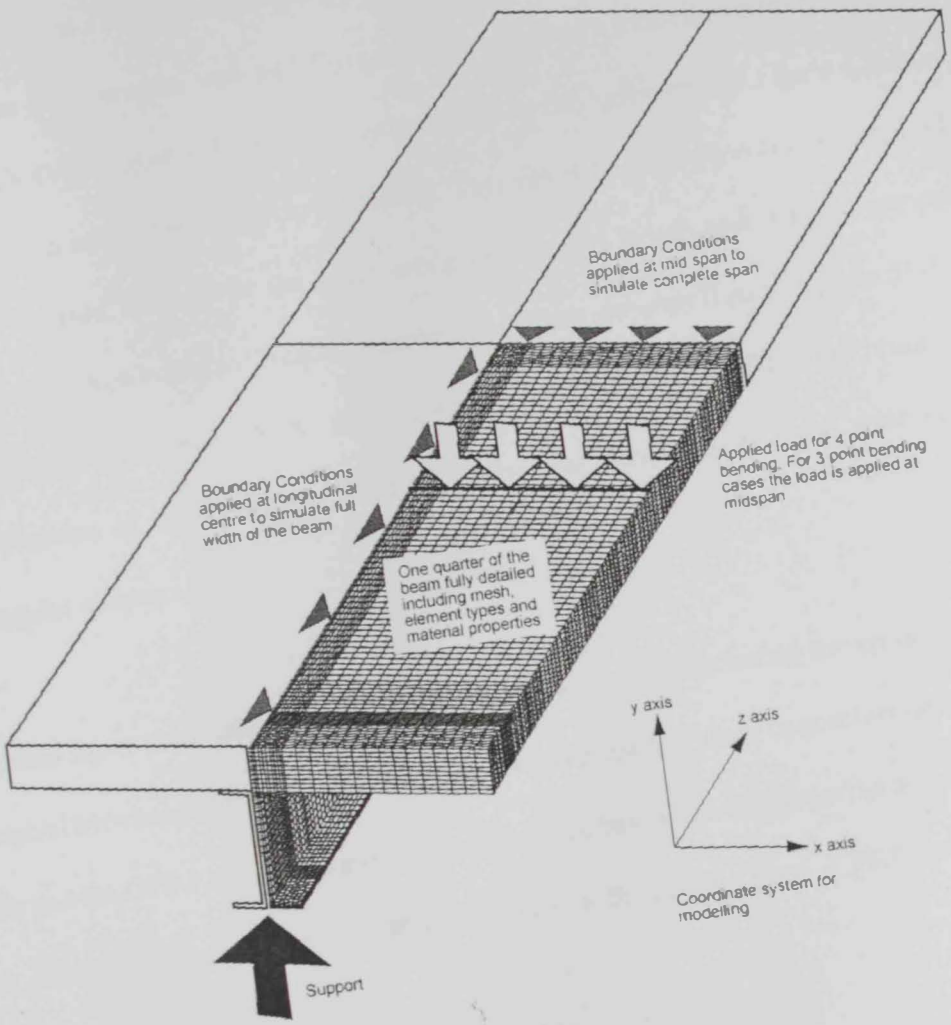

Fig 4.3 *Illustration of the method of modelling in ANSYS. One quarter of the beam is developed in detail and boundary conditions applied at mid span and longitudinal line of symmetry to simulate a full beam. Support points and load points are also shown. The global coordinate system showing x, y and z directions adopted for modelling the geometry is also shown.*

Input parameters

The geometric arrangement of the beam was input based on the actual sizes measured on the tested materials. Some minor simplifications were adopted when modelling the GFRP pultruded section. The physical GFRP specimen had a radius on the inside and outside edges at the join between web and flanges, these radii were modelled with a simple 90° bend in ANSYS. Figure 3.3 shows the actual beam at this position and Figure 4.2 shows the representation of the corner in the model. This simplification permitted a rectangular mesh to be used throughout the beam cross section and length and reduced computer analysis time. According to Oregon Department of Transportation Research paper SPR 316 2001 simplification of a model in this way will not adversely affect the results. No simplification of the concrete or CFRP strips was necessary as these were regular rectangular shapes.

Detailed input parameters were required for each material including the epoxy bonding material between the CFRP and GFRP and the bolts used as shear connectors between the slab and the GFRP beam. The parameters tabulated below are the properties adopted based on laboratory measurements and technical information from CFRP and GFRP manufacturers.

Concrete

The concrete was modelled as element type SOLID 65 (Fig. 4.4). This 3-D 8-noded solid element type is capable of modelling the nonlinear behaviour of concrete, cracking in tension and crushing in compression. The element considers the 3 transitional degrees of

freedom (DOF) i.e. transition in x, y and z directions. SOLID 65 is set up within ANSYS to presume reinforcing is present with reinforcing details input as real constants. The test beams contained only nominal reinforcement therefore the material input for reinforcement was specified as the same properties as the concrete mass, effectively negating any effect of reinforcement steel in the model.

Input parameters for the linear elastic model required elastic Young's modulus (E_{CONC}) and Poisson's Ratio for the concrete material.

Determination of E_{CONC} was based on BS 8110 design code approach of:

$$E_{CONC} = 20 + 0.2\ f_{cu}\ (MPa)$$ BS 8110 : Part 2, Section 7, equation 17

This value is equal to 27,600 MPa. This was found to be satisfactory in previous modelling studies by Fanning (2001). Therefore an E_{CONC} rounded to 28,000 N/mm^2 was selected as an appropriate elastic modulus for the concrete.

The adoption of 0.2 as the value for Poisson's Ratio followed a similar process of using a design code approach verified by independent modelling research. BS 8110 : Part 1, Section 2.4.2.4 recommends a Poisson's Ratio of 0.2 for linear elastic analysis. The Oregon Department of Transportation Research Report SPR 316 2001 confirms this value as appropriate for modelling purposes. Table 4.1 summarises the values discussed above.

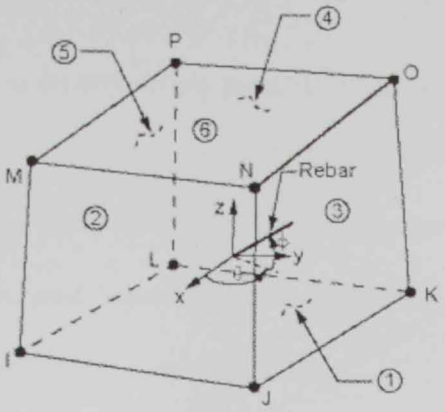

Fig 4.4 *SOLID 65 geometry used as the element type for modelling concrete.*

Concrete Material Properties **Element type SOLID 65**			
Parameter	**Name in ANSYS**	**Value**	**Comment**
Elastic Modulus	Ex	28,000 N/mm^2	From BS 8110 Part 2 and confirmed Fanning 2001
Poisson's Ratio	PRxy	0.2	From BS 8110 Part 2 and confirmed in Oregon Department of Transportation Research SPR 316 2001

Table 4.1 *Isotropic concrete material properties adopted for the numerical model*

Glass Fibre Reinforced Plastic

The GFRP was modelled as an orthotropic material using element type SOLID 64 (Fig. 4.5). This 3-D 8-noded solid element type will model anisotropic materials such as multidirectionally reinforced composites. The element considers the 3 transitional DOF i.e. transition in x, y and z directions. Input of material data for the pultruded sections used in this study defined the GFRP as orthotropic (Table 4.2).

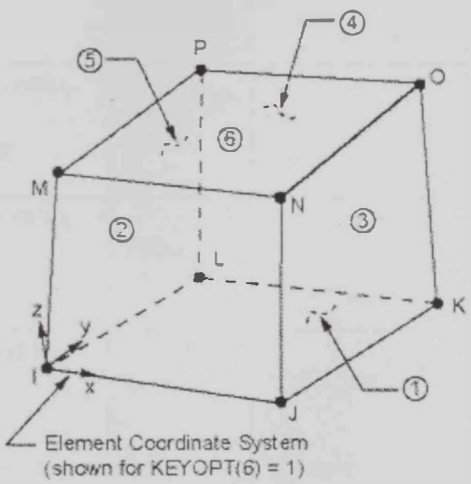

Fig 4.5 *SOLID 64 geometry used as the element type for modelling GFRP and CFRP.*

GFRP Material Properties			Element type SOLID 64	
Constant Number	Parameter	Name in ANSYS	Value	Comment
C1	Elastic modulus, x direction	Ex	3,500 N/mm^2	Based on input from manufacturers literature
C2	Elastic modulus, y direction	Ey	3,500 N/mm^2	Based on input from manufacturers literature
C3	Elastic modulus, z direction	Ez	17,200 N/mm^2	Based on input from manufacturers literature
C4	Poisson's ratio, y-z plane	PRxy	0.3	Based on input from manufacturers literature
C5	Poisson's ratio, y-z plane	PRyz	0.3	Based on input from manufacturers literature
C6	Poisson's ratio, z-x plane	PRzx	0.3	Based on input from manufacturers literature
C7	Shear modulus, x-y plane	Gxy	1,300 N/mm^2	Based on input from manufacturers literature
C8	Shear modulus, y-z plane	Gyz	1,500 N/mm^2	Based on input from manufacturers literature
C9	Shear modulus, x-z plane	Gxz	7,500 N/mm^2	Based on input from manufacturers literature

Table 4.2 Orthotropic GFRP material properties adopted for the numerical model

Carbon Fibre Reinforced Plastic

The CFRP was modelled as an orthotropic material using element type SOLID 64 similar to the GFRP material. Table 4.3 shows the material properties for CFRP.

CFRP Material Properties			Element type SOLID 64	
Constant	**Parameter**	**Name**	**Value**	**Comment**
C1	Elastic modulus, x direction	Ex	3,500 N/mm^2	Based on manufacturers literature
C2	Elastic modulus, y direction	Ey	3,500 N/mm^2	Based on manufacturers literature
C3	Elastic modulus, z direction	Ez	150,000 N/mm^2	Based on manufacturers literature
C4	Poisson's ratio, y-z plane	PRxy	0.3	Based on manufacturers literature
C5	Poisson's ratio, y-z plane	PRyz	0.3	Based on manufacturers literature
C6	Poisson's ratio, z-x plane	PRzx	0.3	Based on manufacturers literature
C7	Shear modulus, x-y plane	Gxy	1,350 N/mm^2	Based on manufacturers literature
C8	Shear modulus, y-z plane	Gyz	1,350 N/mm^2	Based on manufacturers literature
C9	Shear modulus, x-z plane	Gxz	57,700 N/mm^2	Based on manufacturers literature

Table 4.3 Orthotropic CFRP material properties adopted for the numerical model

Epoxy adhesive

Epoxy adhesive was modelled as an isotropic material using ANSYS element type SOLID 64. The layer was modelled as 1.2 mm thick.

The limiting factor on the tested beams was the failure of the bond between the epoxy adhesive and the CFRP. Analysis of this type of fracture or delamination between materials has been the subject of significant studies in recent years. From the traditional methods of fracture analysis other techniques have evolved that adopt softening relationships between tractions and the separations of materials models the energy required to break apart the interface surfacesi This method is known as a cohesive zone approach.

ANSYS has the ability to model the adhesive using a cohesive zone approach using the element type INTER 205. This capacity was not used in this study as the purpose of the numerical model was to simulate behaviour in the linear phase of beam response, therefore a linear elastic element was sufficient.

The elastic modulus and Poisson's ratio applied to the adhesive was obtained from work conducted by Pham and Al-Mahaidi (2004) on bond slip relationships and shown in Table 4.4.

Epoxy Adhesive Properties			Element type SOLID 64	
Constant Number	Parameter	Name	Value	Comment
C1	Elastic modulus	Ex	8,500 N/mm^2	From Pham and Al-Mahaidi
C2	Poisson's ratio	PRxy	0.3	From Pham and Al-Mahaidi

Table 4.4 Epoxy adhesive material properties adopted for the numerical model

Shear connectors

Shear connectors used in the beam were M12 bolt pairs spaced at 50mm cross beam gauge and 125mm centres along the length of the beam. Modelling of these shear connectors became one of the dominating issues in simulating the beam behaviour. ANSYS is able to model the connector as a mass-less spring element with uniaxial tension and/or compression stiffness. This is elastic spring element COMBIN 14(Fig 4.6).

The spring stiffness can be defined along the geometrical longitudinal axis of the element (if the nodes of the element are discrete) or along any global direction. In this study the spring stiffness is defined along the z-direction which is the longitudinal direction of the beam. In the other global directions x and y, every matching node at the concrete to GFRP interface is coupled i.e. will have the same x and y translations.

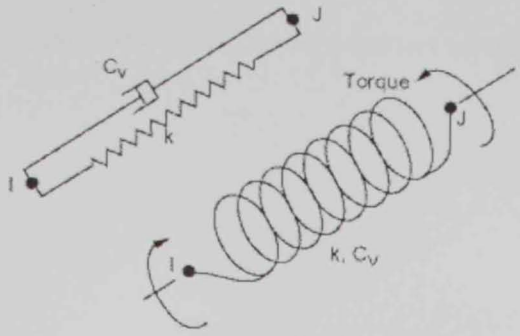

Fig 4.6 *COMBIN 14 geometry used as the element type for the shear connectors between the concrete slab and the GFRP. No damping or torsional stiffness is considered.*

To ensure a reasonable start point for the shear connector parameters and parametric analysis tests specifically simulating the shear connection between the concrete and GFRP were carried out. Inspection of the connectors on all tested beams GFRP, CFRP1 and CFRP2 showed that the GFRP had been deformed around the bolts and that some bolt rotation was evident at the outermost connectors. To simulate this response to load and obtain a value for the spring constant (K) representing the force to extension relationship two shear connector simulation arrangements were adopted.

Connector test arrangement 1 held the shear connector perpendicular to the applied load and resisted rotation in the connector. In this case all the movement was due to deformation in the GFRP due to bearing, therefore providing a measure for the upper bound of K.

Connector test arrangement 2 allowed the shear connector to rotate under load, simulating

more closely what was actually observed in the physical test specimen. These arrangements are detailed in Figure 4.7.

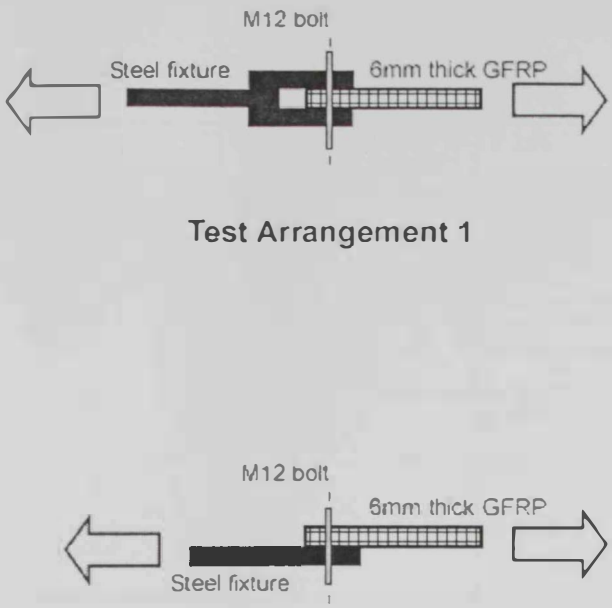

Fig 4.7 *Shear connection stiffness testing arrangement. Test arrangement 1 obtained results for pure bearing without allowing rotation. Test arrangement 2 obtained results for bearing with rotation.*

Plotting the load and extension results to obtain the experimental K value gave the results shown in Table 4.5.

Test Arrangement 1 – Pure bearing with no bolt rotation			
Test connection number	**Load kN**	**Extension mm**	**Spring Constant K N/mm**
11	15	2.4	6,250
11	17.5	3.6	4,861
11	18	5.1	3,529
12	10	1.5	6,667
12	18.5	4.7	3,936
13	10	1.6	6,250
13	18.6	4.8	3,875

Table 4.5 Test results for shear connection with bolts in pure bearing showing spring constant (K) values obtained

It was observed that response to load changed in a series of steps for all samples. An initial stiffness of over 6,000 N/mm was observed up to a first yield point where load capacity was lost and then began to recover offering a K value in this second stage of around 4000 N/mm. This loss and recovery occurred a third time also when the connection was tested to higher loads. This may be attributed to the tensile failure of some filaments and the picking up of load by other filaments which in turn suffer tensile failure.

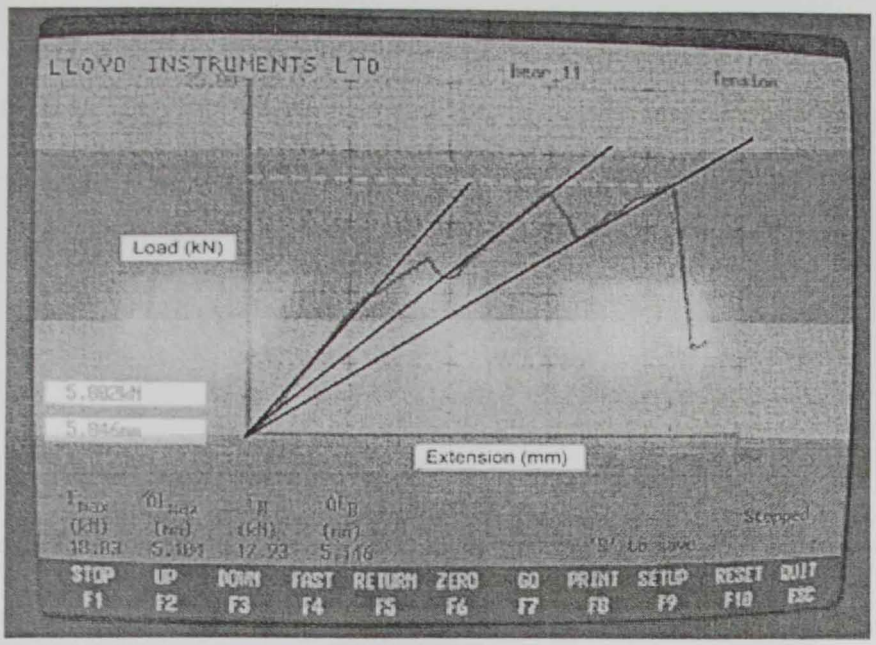

Fig 4.8 *Graphical results of Load verses extension for test sample 11 showing the step changes in graph slope as load increased. The black lines superimposed represent the 3 stiffness or K values obtained from the test.*

Test Arrangement 2 – Bearing with bolt rotation			
Test connection number	**Load kN**	**Extension mm**	**Spring Constant K N/mm**
21	13.17	2.4	4,770
22	20	3.6	5,000
23	20	3.8	5,236

Table 4.6 *Test results for shear connection with bolts in bearing with rotation permitted showing spring constant (K) values obtained*

Unlike test arrangement 1 (the bearing test pieces) the graphs produced for test arrangement 2 were close to straight line all the way to loss of load at which point deformation could be observed due to:-

- Bearing of the bolt on the GFRP
- Rotation of the bolt
- Bending of the bolt

As a result of these tests an average value of 5,000N/mm (Table 4.7) was selected as an appropriate starting point for K in the ANSYS model. This value represented a mid point of the tests that allowed rotation and was lower than the reasonable upper bound provided by the pure bearing values.

Shear Connector Properties			**Element type COMBI 14**
Parameter	**Name**	**Value**	**Comment**
Spring Constant	K	5000 N/mm	Obtained from testing

Table 4.7 Shear connector parameters adopted for the numerical model

Isotropic Input parameters

The fibre reinforced plastics in this beam have a significantly higher elastic modulus in the z direction than in the x and y directions. This property is called orthotropy and is modelled using the parameters given in the preceding sections. In the analysis of these hybrid beams an alternative model using equal properties in (Tables 4.8 and 4.9) x, y and z directions for each material, called isotropy, will be developed for comparison with the orthotropic results.

GFRP Material Properties – Isotropic			**Element type SOLID 64**
Parameter	**Name**	**Value**	**Comment**
Elastic modulus, all directions	Ex	17,200 N/mm^2	The value used is the larger which is in the fibre direction.
Poisson's ratio	PRxy	0.3	

Table 4.8 Isotropic GFRP material properties adopted for the numerical model

CFRP Material Properties – Isotropic			**Element type SOLID 64**
Parameter	**Name**	**Value**	**Comment**
Elastic modulus, all directions	Ex	150,000 N/mm^2	The value used is the larger which is in the fibre direction.
Poisson's ratio	PRxy	0.3	

Table 4.9 Isotropic CFRP material properties adopted for the numerical model

Boundary conditions and loads

The three full size beams were tested using 4 point bending for beam GFRP and three point bending for beams CFRP 1 and 2. The FE models were loaded and supported in the same arrangement and locations as the full size beams. The arrangement of these loads in elevation is shown in Figure 3.6.

The beams all have two planes of symmetry; one at mid-span, mid way between the two supports, and the second is longitudinal along the centreline of the beam. As a result of this symmetry one quarter of the beam was created, meshed and loaded and symmetry boundary conditions applied along the planes of symmetry. A symmetry boundary condition means that out-of-plane translations and in-plane rotations are set to zero for all nodes along the symmetry boundary and the geometry inside the quadrant modelled is reflected with the boundary plane as a mirror plane. Therefore the entire beam, full width and full length can be modelled with the computer time and input only that necessary to complete one quarter of the physical beam. Figure 4.3 shows the beam and the quarter discretised with load, support and boundary symmetry lines shown. Note that the image shows 4-point loading, however the model also used 3-point loading for beams CFRP1 and 2.

4.4 Outline of Parametric Study

A parametric study involves extracting a particular parameter for consideration while all other parameters remain unchanged; in this way the changing of the one parameter permits a clear study of its effect on the behaviour of the beam. In order to bring a convergence of the experimental results with the analytical output a parametric study was carried out on the beams GFRP, CFRP1 and CFRP2 using a range of properties and parameters for each element while the other materials were unchanged. This study enabled the impact of each element on the overall beam behaviour to be analysed.

The parametric study considered the following parameters:-

- Concrete elastic modulus (E_{CONC})
- Shear connector stiffness (K)
- GFRP elastic modulus (E_{GFRP})
- CFRP elastic modulus (E_{CFRP})

Each parametric analysis run uses an applied total load of 50kN.

The base properties used for the start point of each analysis are as follows unless otherwise noted:-

- Concrete elastic modulus (E_{CONC}) 28,000 N/mm^2
- Shear connector stiffness (K) 5,000 N/mm
- GFRP elastic modulus (E_{GFRP}) strong, stiff direction 150,000 N/mm^2
- CFRP elastic modulus (E_{CFRP}) weak direction. 17,200 N/mm^2

Concrete Elastic Modulus

The concrete property dominating the strains and the deflection of the beam is the elastic modulus. Determination of E_{CONC} was based on BS 8110 design code approach. This was reported to be satisfactory in previous modelling studies by Fanning (2001), therefore an E_{CONC} of 28,000 N/mm^2 was selected as an appropriate start point based on the compression strength tests for the actual concrete used. The range of Elastic modulus values in the parametric study start from a minimum point of 5,000 N/mm^2 to a maximum of 50,000 N/mm^2.

Shear Connectors Stiffness

The property governing the behaviour of the shear connectors is the assigned spring constant (K) representing the load to deformation ratio in N/mm. Testing of isolated connections as reported in this paper indicate a K value of 5000 N/mm to be appropriate. The range of K values in the parametric study begins from a minimum point of 10 N/mm to a maximum of 50,000 N/mm

GFRP Elastic Modulus

The glass fibre reinforced plastic property dominating the strains and the deflection of the beam is Elastic modulus. Manufacturer's data indicates that an E_{GFRP} of 17,200 N/mm^2 was an appropriate start point. The values used for E_{GFRP} in the parametric study range from 5,000 N/mm^2 to a maximum of 40,000 N/mm^2.

CFRP Elastic Modulus

The carbon fibre reinforced plastic property dominating the strains and the deflection of the beam is elastic modulus. Manufacturer's data claims an E_{CFRP} of 150,000 N/mm^2 was an appropriate start point. The values used for E_{CFRP} in the parametric study range from a minimum of 50,000 N/mm^2 to a maximum of 500,000 N/mm^2.

4.5 General Behaviour of Composite Beams:

Based on common knowledge of the behaviour of thin or shallow elastic non-composite beams, the strain profile across the beam's cross section is linear and continuous (Fig. 4.9). On the other hand, the strain profile for a thin composite beam is piece-wise linear and has discontinuities at the interfaces between any two connected layers of the composite beam (Fig. 4.10). For the same curvature for the two layers, the strain linear segments should be parallel. If the beam layers are to behave separately, each layer will have its own neutral axis for the strains. It is the increasing stiffness of the shear connector between the two layers who brings these two separate neutral axes closer.

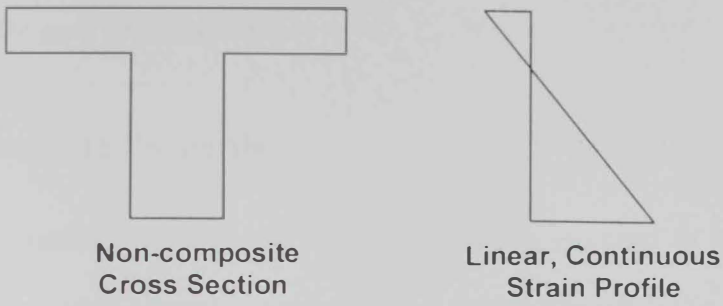

Fig. 4.9 *Cross-section and continuous strain profile for non-composite sections*

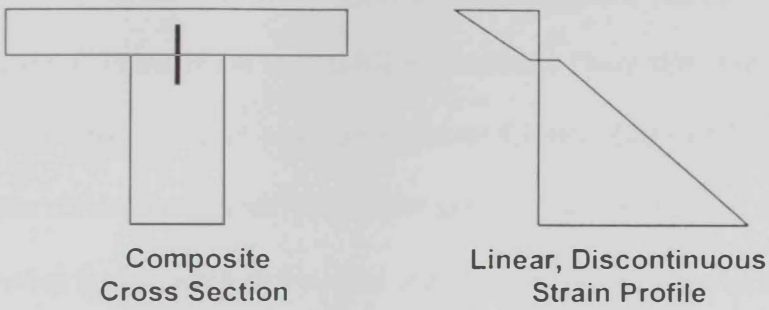

Fig. 4.10 *Cross-section and discontinuous strain profile for composite sections*

It is also evident that the non-composite cross section shown in Fig. 4.9 is stiffer (i.e., has a larger value for EI, where I is the cross-sectional moment of inertia) than the composite section in Fig. 4.10. Therefore, this non-composite section is expected to exhibit less strain than the composite one, for the same bending moment. Since deflection is inversely proportional to the stiffness of the beam cross section, for the same load values and pattern, it is expected that the beam with cross section given by Fig. 4.9 exhibits less deflection than a beam with cross section given by 4.10 provided that the load values and pattern is the same.

This basic introduction about the behaviour of composite beams will help explain the results of the Finite Element analysis conducted in this study.

4.6 Results and Discussion

Effect of Concrete Properties

The parametric analysis varying the value of the elastic modulus of concrete from a minimum value of 5000 N/mm^2 to a maximum of 50,000 N/mm^2 , while all other values remained unchanged from their base properties, produced a series of graphs showing the effect E_{CONC} on the strains predicted at the beam cross-section at the mid-span and at the symmetry line between the two GFRP channels. The graphs also shows the spring forces applied to the shear connectors at the slab/GFRP interface. These effects are shown in Fig. 4.11 which shows the effect on beam arrangement CFRP1. Beams GFRP and CFRP2 produce similar results. From a review of these graphs it can be observed that:-

- Increasing E_{CONC} increases the beam overall stiffness leading to lesser strains, mid span deflection, and overall curvature. This is usually accompanied by reduction in the slip strain (difference between the strains at the concrete/GFRP interface)
- Since increasing E_{CONC} reduces the beam curvature and corresponding deflection, it will also reduce the forces in the shear connectors.
- Increasing/reducing E_{CONC} moves the neutral axes in the two different material slightly.
- For the shown case of beam CFRP1, the portions of the strain profile for the top concrete part and the lower part of the beam are linear but no parallel. This is contradicting the basic concepts discussed earlier which are based on the well established behaviour of thin beams. On the contrary, the results for the beam GFRP show parallel strain segments which agrees better with the thin beam theory. After careful investigation it is found that for the beams CFRP1 and CFRP2, with

high tensile capacity, the compressive stresses and strains across the width of the concrete flange are not uniformly distributed but show a significant peak at the centre of the section and decays as the location departs from the centre toward the edges of the flange.

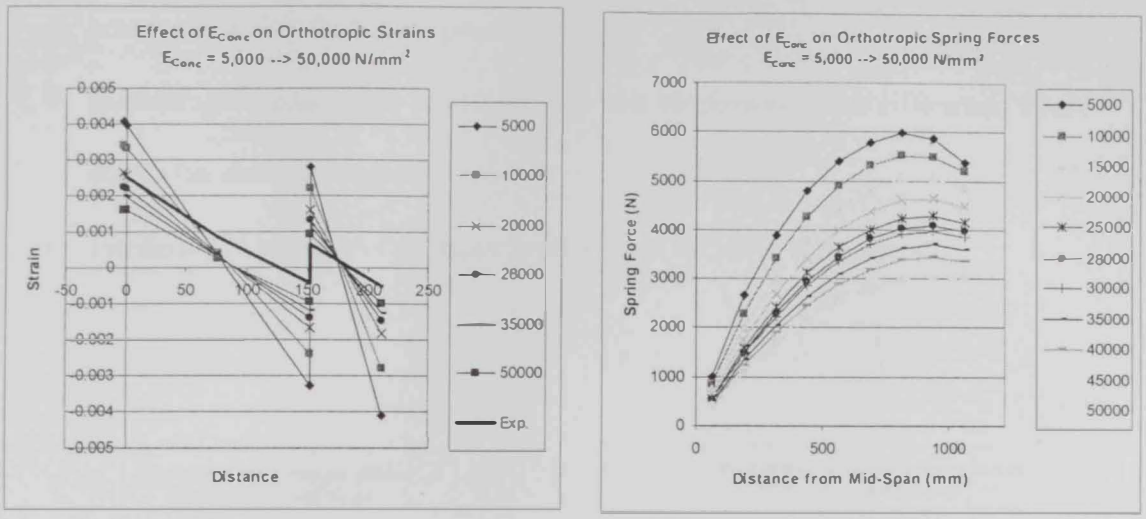

Fig 4.11 *Graphical results for Beam CFRP1 showing the effect of variations in E_{CONC} on strains and spring forces at shear connectors*

Shear Connector Properties

The parametric analysis varies the spring (stiffness) constant of the shear connectors K from a minimum value of 10 N/mm to a maximum of 50,000 N/mm. This covers a wide range that represents extremes of K from close to zero to approaching a solid connection. The analysis produced a series of graphs showing the effect of changing K on the strains predicted at the beam mid-span and on the spring forces developed in the shear connectors. These effects on beam arrangement CFRP1 are shown in Figure 4.12. From a review of this

graph and results for beams GFRP and CFRP2 it can be observed that:-

- Increasing K brings the two neutral axes of the beam's two layers closer which represent an increase in the composite action in the beam leading to a larger stiffness and lower deflection. It is clear that K=50,000 N/mm (which is about 10 times the estimated stiffness for the shear connectors) is not enough to develop full composite action that corresponds to K= ∞.
- Increasing K reduces the interfacial slip and consequently the differential strain across the shear connectors.
- Increasing K increases the forces developed in the shear connectors.

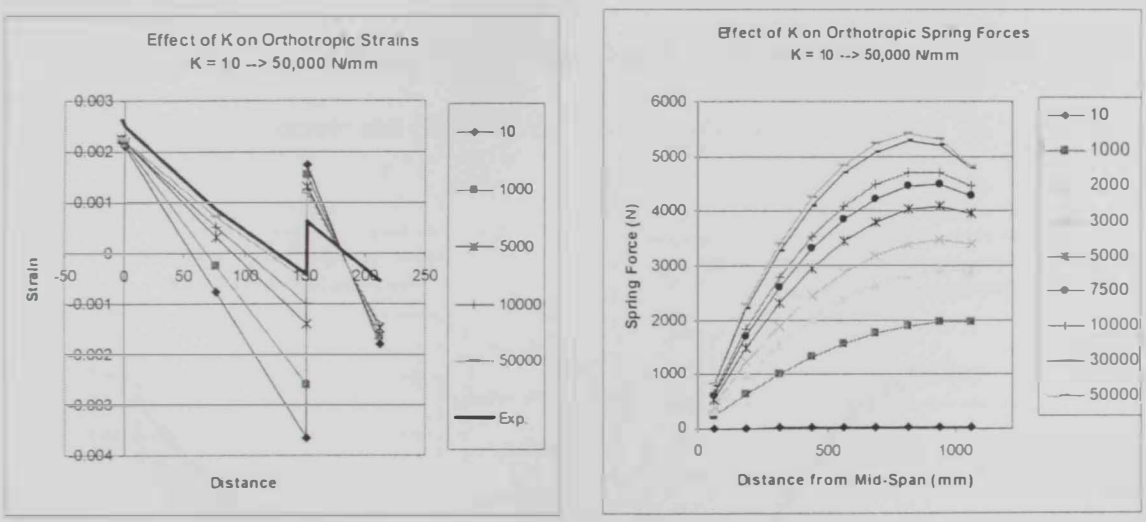

Fig 4.12 *Graphical results for Beam CFRP1 showing the effect of variations in spring stiffness K on strains and spring forces at shear connectors*

GFRP Properties

The parametric analysis varying the value of the elastic modulus of the GFRP from a minimum value of 5000 N/mm^2 to a maximum of 40,000 N/mm^2 produced a series of graphs showing the effect E_{GFRP} has on the strains predicted at the beam mid-span and the spring forces applied to the shear connectors. These effects on beam arrangement CFRP1 are shown in Figure 4.13. From a review of this graph and results for beams GFRP and CFRP2 it can be observed that:-

- Since the area and moment of inertia of the GFRP component is relatively small when compared to the concrete, increasing E_{GFRP} increases slightly the overall stiffness of the beam, reduces strains, and reduces slightly the mid span deflection. Therefore reduces slightly the forces applied to the shear connectors.
- Increasing E_{GFRP} reduces slightly the change in differential strain across the interface of concrete and GFRP at the shear connectors.

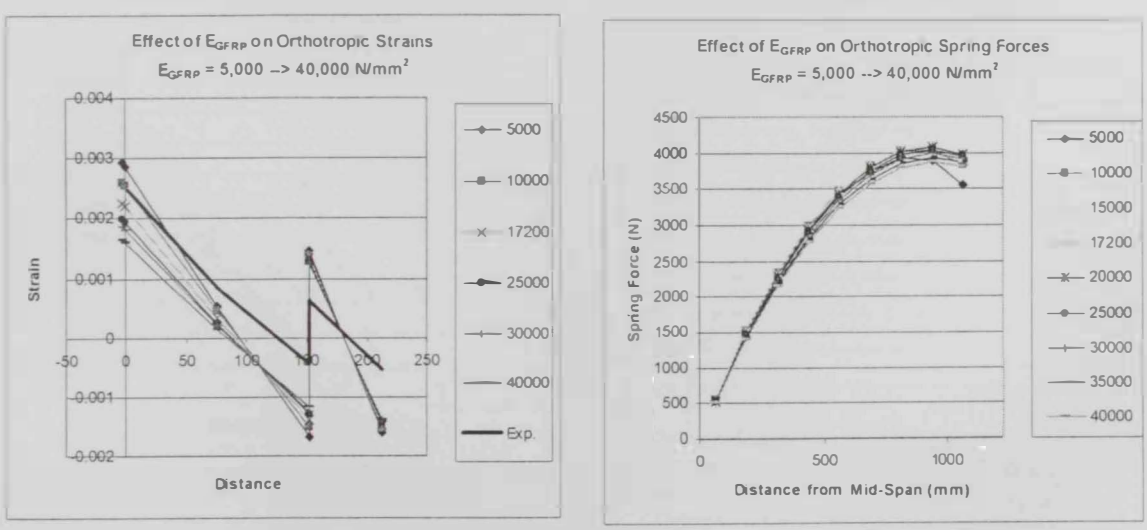

Fig 4.13 *Graphical results for Beam CFRP1 showing the effect of variations in E_{GFRP} on strains and spring forces at shear connectors*

CFRP Properties

The parametric analysis varying the value of the elastic modulus of the CFRP strip from a minimum value of 50,000 N/mm^2 to a maximum of 500,000 N/mm^2 produced a series of graphs showing the effect E_{CFRP} has on the strains predicted at the beam mid-span and the spring forces applied to the shear connectors at the slab/GFRP interface. These effects on beam arrangement CFRP1 are shown in Figure 4.14. From a review of this graph and results for beams GFRP and CFRP2 it can be observed that:-

- Increasing E_{CFRP} reduces the strains at the CFRP layers significantly, which consequently affects the strains in the GFRP portion of the beam leading to a moderate control over the deflection.
- Increasing E_{CFRP} slightly affects the strain in the concrete.
- Increasing E_{CFRP} has negligible effect on forces applied to the shear connectors.

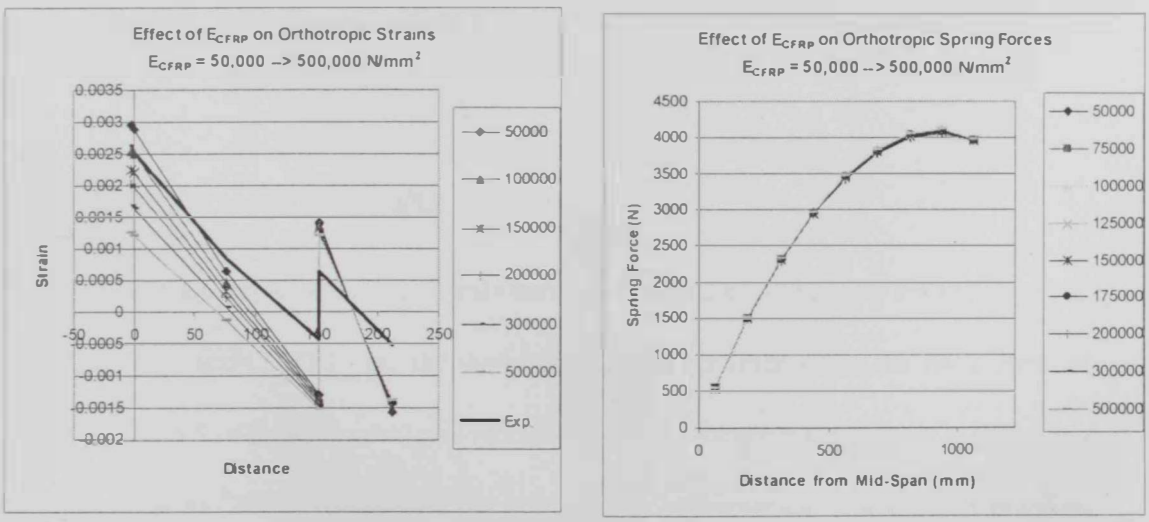

Fig 4.14 *Graphical results for Beam CFRP1 showing the effect of variations in E_{CFRP} on strains and spring forces at shear connectors*

Material Interactions

Reviewing the trends observed and represented on graphs 4.11 to 4.14 it can be observed that particular aspects of the beam behaviour are affected more dramatically by certain materials. Specific and general effects of changing material properties are as follows:-

- The concrete elastic modulus controls significantly the strain profile across the beam cross-section.
- The shear connectors' stiffness K is the primary determinant of differential strain at the interface of the slab and GFRP and the forces in the shear connectors. It also affects the strains in the GFRP portion and CFRP layers. It has very little effect on the concrete strains at the variation levels we have reviewed.
- The CFRP elastic modulus affects the strain in the entire CFRP layers and the GFRP portion of the beam, especially at the CFRP level, but has little effect on the concrete strains.
- Changes to the E_{GFRP} produce a small change in the connector forces

4.7 Comparison of Results

In this section a comparison is made between the observed experimental results of beams GFRP, CFRP1 and CFRP2 and the theoretical results obtained using the finite element program ANSYS in order to verify the numerical model. An approach similar to that taken by Queiroz et al (2006) considered the comparison of numerical results with physical testing observations over four points of measurement have been used.

- Comparison of deflection at mid span
- Comparison of the negative strains at the top surface of the concrete slab.

- Comparison of the negative strains at the top surface of the GFRP. This does not give us the complete picture of structural action at this interface position where the strain change is more applicable, however strains were not physically measured at the underside of the concrete during testing.
- Comparison of the positive strain at the underside of the GFRP
- Comparison of the positive strain at the underside of the CFRP

In addition to verifying the numerical model this approach will identify how sensitive the beam arrangement is to changes in material properties.

The datum point for properties for the numerical model as described in section 4.4 were:-

E_{CONC}	28,000 N/mm^2
E_{GFRP}	150,000 N/mm^2
E_{CFRP}	17,200 N/mm^2
Shear connector stiffness (K)	5,000 N/mm

Mid span deflection

In this section a comparison and analysis is made of the measured and calculated deflections. Mid span deflections measured at 50kN load during the experimental work can be compared with numerically modelled deflections. The effect of variations in material properties on deflection has been mapped against measured experimental results and shown on the graphs in figure 4.15.

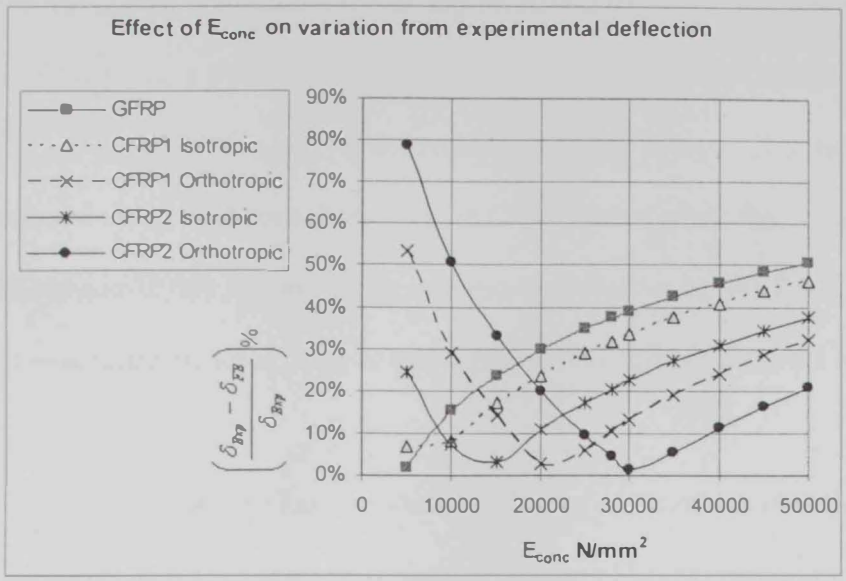

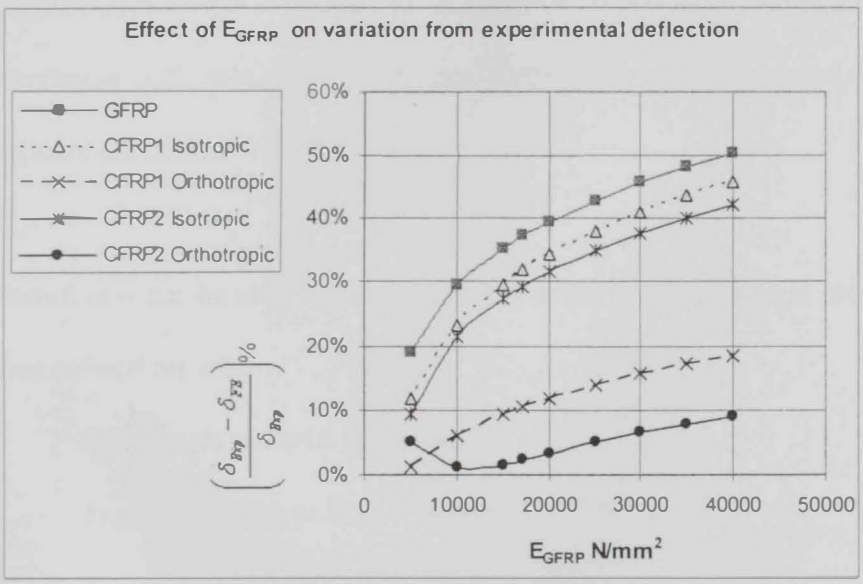

Fig 4.15 *Graphical results showing the effect of variations in E_{CONC} and E_{GFRP} for all modelled beams when compared with the experimentally measured mid span deflection.*

From these results it can be seen that while leaving the material properties for GFRP, CFRP and the spring constants fixed at the initial values and varying the concrete material property E_{CONC} a good match of experimental and theoretical deflections can be selected. The initial point of E_{CONC} was determined as 28,000 N/mm^2. This appears to match well with the theoretical deflection for both CFRP beams when the E_{CONC} value is between 20,000 and 30,000 N/mm^2. Using orthotropic properties of GFRP and CFRP provides the more accurate model as using isotropic properties underestimates the mid span deflection.

The GFRP section also has a secondary influence on the mid span deflection of the beam.. The results indicate that the manufacturer's claim of 17,200 N/mm^2 for elastic modulus for the pultruded GFRP is reasonable. A range of 10,000 to 20,000 N/mm^2 returns a good correlation with measured deflections. Orthotropic material models provided a more accurate prediction of deflections

Therefore is can be seen that the numerical model provides a good prediction of the mid span deflections when:

Orthotropic material properties are used

E_{CONC} of 20,000 to 30,000 N/mm^2

E_{GFRP} of 10,000 to 20,000 N/mm^2

Top of Concrete Strains

Negative strains measured at the top of the concrete slab at 50kN load during the experimental work can be compared with numerically modelled strains. It has been observed that the material property that most influences the strain at this point is E_{CONC}, while E_{GFRP} and the shear connector constant K have very small effects. E_{CFRP} has almost no effect at this point. Strain measurement from specimen GFRP provided the value of strain at a position of 150mm off the beam mid span position. To obtain mid span strain the measured value was linearly extrapolated by multiplying by the ratio of distances from the support, i.e.1025mm/875mm.

The effect of variations in the concrete material property E_{CONC} on strain has been mapped against measured experimental results and shown on graphs in Fig 4.16.

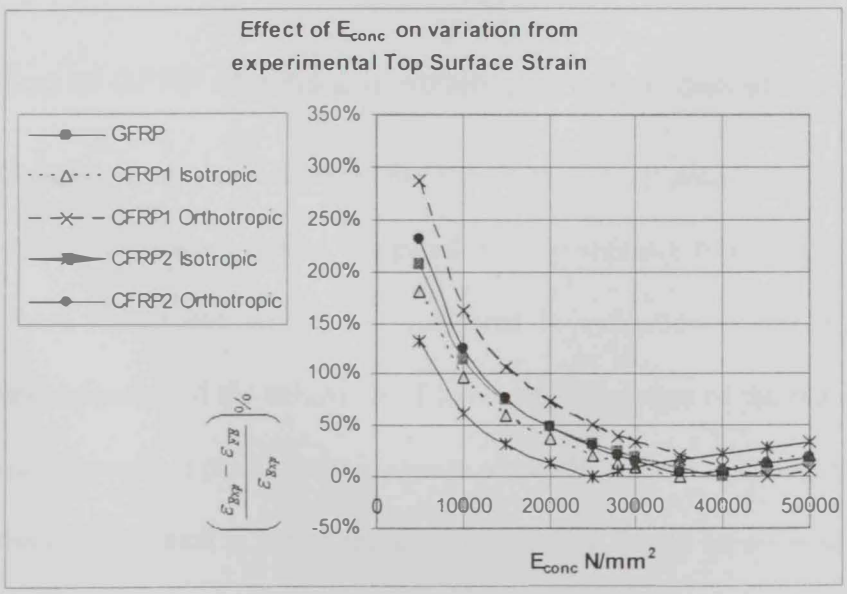

Fig 4.16 *Graphical results showing the effect of variations in E_{CONC} for all modelled beams when compared with the experimentally measured top of concrete strain.*

From these results it can be seen that while leaving the material properties for GFRP, CFRP and the spring constants fixed at the initial values and varying the concrete material property E_{CONC} an optimum match point of experimental and theoretical deflections can be selected however the accuracy of the predicted strains is not high. Strains appear to match best with the theoretical predictions for all beams when the E_{CONC} value is between 25,000 and 45,000 N/mm^2, the value of best fit for all beams is approximately 40,000 N/ mm^2 Within the range of E_{CONC} suggested by mid span deflection comparisons, i.e. 20,000 to 30,000 N/mm^2, the theoretical strain is generally overestimated by up to 40%.

In reviewing these points it can be considered that an elastic modulus of 25,000 to 35,000 N/mm^2 for the concrete provides a reasonable prediction of the mid span strains on the top of the concrete, however the level of accuracy of accuracy is approximately +40% to -25%.

Top of GFRP strains and strain change across shear connectors

Negative strains measured at the top of the GFRP section at 50kN load during the experimental work can be compared with numerically modelled strains from ANSYS. These results can be directly compared in validation of the model. For a clearer understanding of the behaviour of the composite action of the beam and its elements a measurement of the total strain change across the interface between the concrete slab and the GFRP, which is across the shear connectors, would be more beneficial. During the testing phase actual strain readings were not taken at the underside of the concrete therefore the experimental value of strain change cannot be obtained and direct comparison is not possible.

When only the strains at the top of the GFRP are considered it has been observed that the material property that influences the strain at this point most significantly is the stiffness of the shear connectors. E_{CONC} and E_{GFRP} exert lesser influences respectively while E_{CFRP} has almost no effect. This position is characterized by large differences in the actual and theoretical strains for all of the beam arrangements. In all cases the strain is overestimated in the numerical model.

The effect of variations in K on negative strain has been mapped against measured experimental results and shown on the following graphs in Fig 4.17.

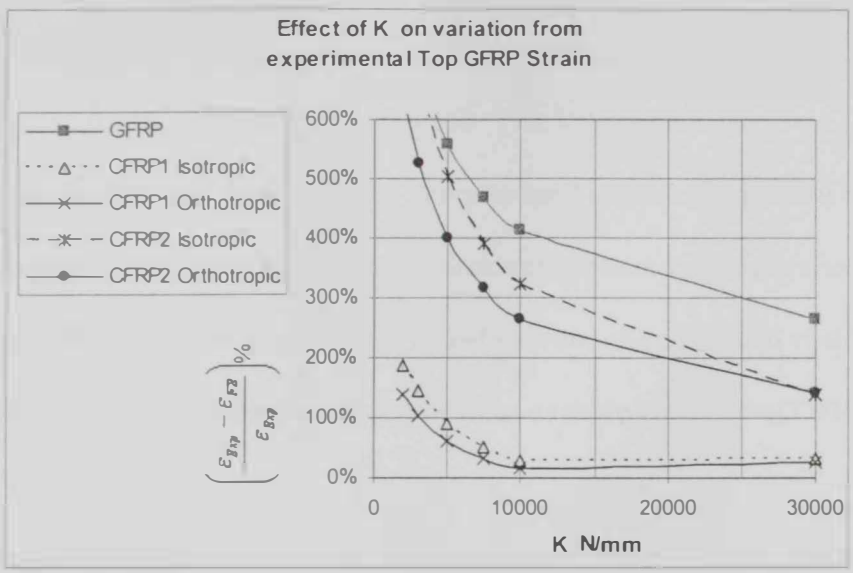

Fig 4.17 *Graphical results showing the effect of variations in K for all modelled beams when compared with the experimentally measured top of GFRP strain.*

Two observations can be made from the trends shown in this graph. Firstly that the curve is very steep over the range of K from zero to 10,000 N/mm. This indicates a high sensitivity in top GFRP strains to variations in K, particularly in the range of values around 5,000

N/mm therefore making it difficult to obtain agreement with measured strains. Secondly that numerical model values for beam CFRP1 showed better agreement with experimental results than all other beams.

When considering the total strain change across the shear connectors it is necessary to calculate the theoretical value of the strain at the underside of the concrete slab. Using classical beam theory whereby plane sections remain plane the underside of concrete strain is calculated from the strain at the top of the concrete and the slope of the strain line observed within the depth of the GFRP section. It must also be considered that concrete cannot reliably sustain tension. BS 8110 provides guidelines for maximum flexural tension

$0.45 f_{cu}^{½}$ (MPa) BS 8110 : Part 1, Section 4

This equates to 2.8 MPa for the concrete used in the experimental beams. This further complicates the consideration of underside of concrete values calculated however it can be seen from a review of numerical model data and the calculated strains that the trends at underside of concrete are broadly the same as those at the top of GFRP.

Agreement between modelled and measured values is not good, however the value of K = 5000kN/mm can be adopted with confidence due to the independent testing carried out.

Underside of GFRP Strains

Positive strains measured at the underside of the GFRP section at 50kN load during the experimental work were compared with numerically modelled strains. It was observed during the parametric analysis that three material properties influenced the strain at this

point. E_{CFRP}, E_{CONC} and to a slightly lesser extent E_{GFRP} all influence the strain at the underside. The shear connector constant K has almost no effect.

The effect of variations in the material properties E_{CONC}, E_{CFRP} and E_{GFRP} on strain has been mapped against measured experimental results and shown on the following graphs.

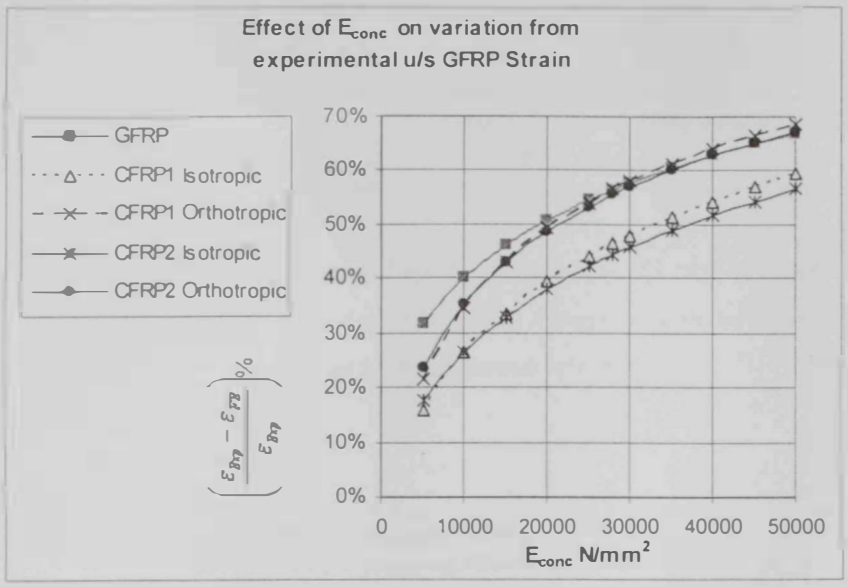

Fig 4.18 *Graphical results showing the effect of variations in E_{CONC} for all modelled beams when compared with the experimentally measured strains at the underside of GFRP.*

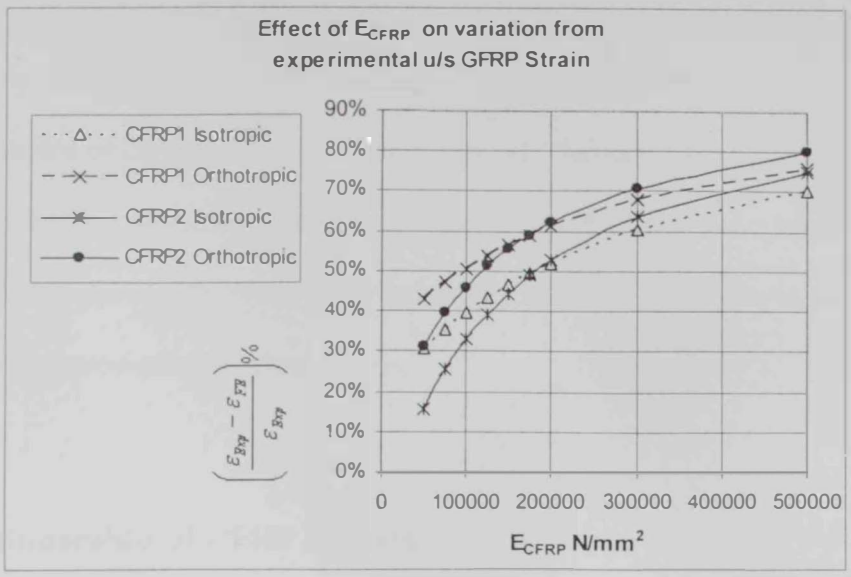

Fig 4.19 *Graphical results showing the effect of variations in E_{CFRP} for all modelled beams when compared with the experimentally measured strains at the underside of GFRP.*

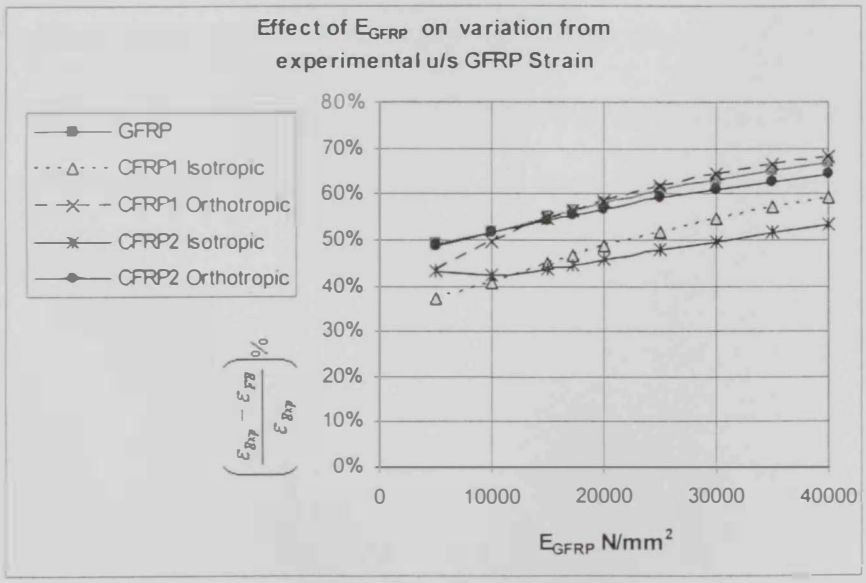

Fig 4.20 *Graphical results showing the effect of variations in E_{GFRP} for all modelled beams when compared with the experimentally measured strains at the underside of GFRP.*

From these results it can be seen that the beam will be most sensitive to the E_{CFRP} value as the graph is steepest over the range 100,000 to 200,000 N/mm^2 which is the magnitude quoted by the manufacturer for this material. The comparison of calculated to experimental gives a consistent match within 40 to 60%. The calculated value consistently underestimates the strain at the underside of the GFRP. Isotropic material models provide a better prediction of actual strains.

Underside of CFRP Strains

Positive strains measured at the underside of the carbon reinforced plastic strip at 50kN load at mid span during the experimental work was compared with numerically modelled strains at the same point. It has been observed that the primary material properties that determine the strain at this point are E_{CONC} and E_{CFRP}. E_{GFRP} has a lesser effect and the shear connector constant K has almost no effect at this point.

The effect of variations in the concrete material property E_{CONC} on strain has been mapped against measured experimental results and shown on the following graphs in Fig 4.21.

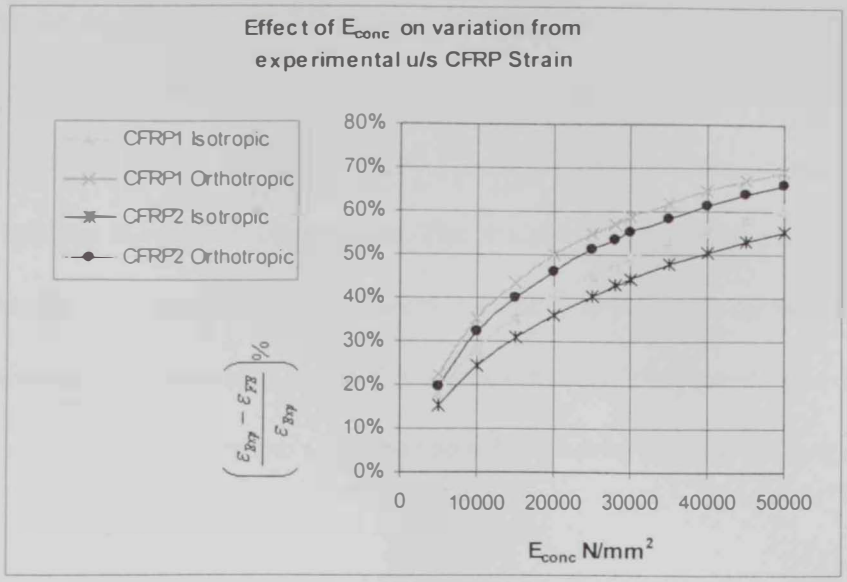

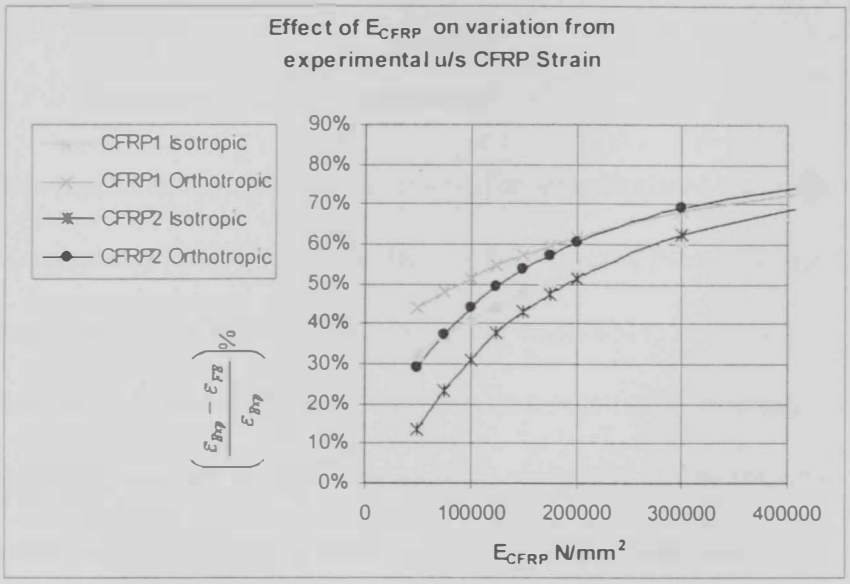

Fig 4.21 *Graphical results showing the effect of variations in E_{CONC} and E_{CFRP} for all modelled beams when compared with the experimentally measured strains at the underside of CFRP.*

From these results it can be seen that while leaving the material properties of the materials not being considered and the spring constants fixed at the initial values that the analytical results are within 35%-55% of measures strains. The calculated values are consistently lower than measured strains. The calculated strains show an increased sensitivity to variation in E_{CFRP} at lower values. The strains are less sensitive to changes in E_{CONC}.

In this case the orthotropic strains are the less accurate of the pairs for each beam arrangement, returning lower strains at each calculation point. The differences between orthotropic and isotropic values are broadly consistent across the range of elastic modulus values calculated.

4.7 Summary and Conclusions

This chapter has reviewed the problem of creating an elastic numerical model with ANSYS in an attempt to accurately simulate the behaviour of the beams under study in the linear elastic portion of the loading curve. After establishing material parameters a parametric analysis was carried out to provide data on trends and in an attempt to fine tune material properties in order to obtain an accurate simulation of the response of the actual beam behaviour. A review of each material and its trends and effects resulted in these conclusions:

- E_{conc} affects all points within the beam cross-section and dominates defection and top surface strain. Increasing E_{CONC} reduces both deflection and top surface strain. A value of 28,000 N/mm^2 for E_{CONC} is close to the BS 8110 guideline and provides reasonable compatibility with actual values.

- Shear connector stiffness (K) is a significant contributor to the differential strains at the concrete/GFRP interface. In addition as K increases the loads predicted on the shear connectors increase in proportion. The effect of K is limited elsewhere in the beam section. Strains at top of GFRP appear highly sensitive to K variations however a value of 5,000 N/mm was established through tests and does not appear unreasonable when reviewing the results of the parametric analysis.

- GFRP properties affect deflection and has an effect on every point measured throughout the beam depth. An increase in E_{GFRP} reduces the magnitude of strains and deflection and reduces the forces on the shear connectors. A value of 17,200 N/mm^2 as claimed by the manufacturer seems to provide a reasonable match of calculated to actual mid span deflections. Matching of strains at top and bottom of the GFRP section which are significantly influenced by E_{GFRP} could not be so well achieved with a consistent underestimate of the magnitude in the order of 35 to 60%. This is possibly due to the sensitivity of the strains to small changes in the value of K.

- CFRP properties affect predominantly the strains at the bottom of the CFRP and GFRP and slightly effect mid span deflection. Increasing E_{CFRP} reduces strain magnitudes throughout the section and reduces deflection. E_{CFRP} had no effect of shear connector forces. Calculated strains were within approximately 60% of measured strains.

Both orthotropic and isotropic properties were considered for the fibre reinforced materials.

Comparison of numerical calculations for each of these alternatives with the experimental results yielded the following:

- Orthotropic properties more accurately simulated deflections.
- Orthotropic properties consistently underestimated strains at all points on the beam section, however both orthotropic and isotropic analysis was subject to errors in the order of 30 to 60% while the difference between orthotropic and isotropic predictions was generally much less than this amount, often around 10%.
- Orthotropic and isotropic analysis consistently showed the same trends.

The numerical program as developed in this paper achieved a reasonable convergence with the actual measured values within the scope of experimental error when critical material properties within these ranges:

- Elastic Modulus concrete 20,000 - 30,000 N/mm^2
- Stiffness coefficient of shear connectors 5,000 N/mm
- Elastic Modulus GFRP 10,000 – 20,000 N/mm^2
- Elastic Modulus CFRP 100,000 - 150,000 N/mm^2

Within the material parameters above validation of the numerical model was achieved when compared with the 4 measurement points:

- Deflections at mid span were consistent with measured values of all three beams within an accuracy level of 35%. Orthotropic properties improved simulation to within 15% of actual deflections
- Top of concrete slab strains were consistent with measured values within 35%,

using isotropic material parameters improved the accuracy.

- Top of GFRP strains were poorly matched with actual figures. Beam GFRP1 provided the best match with 50 to 80% error.
- Bottom of GFRP strains matched consistently but with an under estimation of strain in all beams of 30 to 60%
- Bottom of CFRP strains again matched within 30 to 60% with a consistent under estimation of the magnitude of the strain.

At this point the numerical model will simulate the general behaviour within the linear range of the composite hybrid beams that have been studied. Moving the analysis into non-linear regions will provide more information on the performance and failure models of this material and special arrangement. Non-linear analysis of these beams up to the maximum tested loads was explored but not pursued in depth because the span to depth ratio of the beam specimens as tested was approximately 9.5. This meant that the beams were not strictly thin beams and therefore shears within the structure would begin to play a more influential role, particularly at high loads. Difficulties in modelling of this phenomenon would complicate the analysis beyond the scope of this study.

Suggestions for improvements

While these results are satisfactory there are simple steps that could have been taken that would have eased the process of comparison and validation of the numerical model. The most simple of these is to install more strain gauges. A strain gauge at the underside of the concrete slab and 2 gauges at each position would have improved the level of certainty

when comparing analytical and experimental results. Secondly, the construction of more beams of the same arrangement as those used would have provided additional data and therefore better certainty.

Future experimental studies should increase the span to depth ratio to above 15 to minimize the effect of shear deformations on the overall beam behaviour.

CHAPTER FIVE: SUMMARY AND CONCLUSIONS

CHAPTER FIVE: SUMMARY AND CONCLUSIONS

5.1 Summary

The purpose of this study was to observe the flexural performance of hybrid composite beams using concrete in compression, CFRP in tension and GFRP between the two using physical testing as the primary method of data acquisition. This study particularly observed the effect of different amounts of carbon fibre placed on the tension face of the beam for comparison with beams with no CFRP.

In the experimental stage three 2-metre long test specimens were manufactured, one with no CFRP, one with one strip of CFRP and the third with 2 strips. These were tested in flexure up to failure, strains and deflections were recorded at critical points of the mid span section.

In addition a finite element numerical model was developed to model the behaviour of the beam and materials under flexural loading in the linear elastic range of beam response. The geometry and loading were simple to model, however several difficulties needed to be overcome in modelling the materials. Three different materials and two different material interfaces gave plenty of opportunity for error. Therefore a parametric analysis, including material properties and variations in the shear connection stiffness between concrete and GFRP elements, was carried out to confirm the property values adopted and to test the sensitivity of the model to various material property changes.

In order to validate the numerical model results the outputs for each beam arrangement were compared with those obtained in the experimental study.

The study successfully tested the beams and completed a finite element program that simulated beam behaviour with a reasonable degree of accuracy. The model may be developed further into the nonlinear regions of material response.

5.2 Conclusions

The results of the experimental and theoretical analysis of the flexural behaviour of hybrid composite beams can be summarized and the following conclusions drawn:

- The addition of CFRP to the underside of the composite concrete and GRFP beam provides an improvement in load carrying capacity (i.e., bending strength) and a benefit in deflection control over beams without CFRP.
- The means of securing of larger amounts of CFRP to the beam is significant in gaining full benefit from the CFRP. In this experiment addition of a second layer of CFRP did not produce the full benefit. This was attributed to the method of fixing.
- The use of adhesive to bond the CFRP to the GFRP provides a potential weakness in the hybrid system and an additional difficulty in construction as this is highly sensitive to the quality of workmanship during fabrication or construction.

- Failure by de-bonding of the CFRP was sudden, giving the failure mode a brittle nature.
- The finite element numerical model can predict beam deflections and material strains with reasonable accuracy within the linear elastic range of beam response in the arrangements studied. Although the model did not return highly accurate results, it is still capable of providing reasonable detailed data at any point throughout the beam and so can be considered a powerful tool in analyzing the general performance of hybrid beams. It can also be reasonably expected that the model may be further developed to model the non-linear regions of beam behaviour and failure.

5.3 Recommendations for Future Research

On completion of the experimental and theoretical work in this study it became clear that there were areas that were applicable to this topic that would be worthy of dedicated study. There are also suggestions on how to better establish data when further experimental work is to be carried out and there are a few more good ideas inspired by the process of learning. These then are suggested

- More strain gauges and LVDTs should be installed along the beam length and width to study the strain profiles at different sections and to measure slip along the concrete-GFRP interface.

- Future experimental studies should be more specific in selection of span to depth ratio. Either increase the span to depth ratio to above 15 to operate in more pure flexure and reduce the contribution of shear deformations, or reduce the ratio to be more clearly in a deep beam scenario.
- The shear connection between GFRP and the concrete slab is the element in this structure that will be most subject to corrosion. Studies on methods of providing good shear connection with a non ferrous material would improve the viability of the hybrid structures in marine, coastal or other corrosive environments. The predictability of the stiffness coefficient provided by such arrangements is also important as it has a major effect on the top surface strains in the GFRP and the composite action in general.
- The finite element analysis is recommended to be extended to include non-linear beam response and failure prediction, although it is clear from this study that it is a difficult job.
- As CFRP is the most expensive element in the structure the completed numerical model would enable studies to investigate the amount of CFRP for various arrangements of material and optimize this element.

- The tests carried out in this study did not include any consideration of long term creep effects which are frequently a limitation of reinforced plastic structures. More experimental studies are needed to investigate these creep effects on the hybrid beam arrangement.

REFERENCES

ACI 318-95 *Building code requirements for structural concrete.* ACI Manual of Concrete Practice Part 3: Use of concrete in Buildings – Design, Specifications, and Related Topics. Detroit, Michigan; 1996

Al-Amery, R., Al-Mahaidi, (2006) *R. Numerical analysis of multilayered CFRP RC beams with partial interaction.* Composite Structures Volume 75, Issues 1-4 , September 2006, Pages 479-488, Thirteenth International Conference on Composite Structures - ICCS/13

Barbosa, A. F., Ribeiro, G. O. (1998) *Analysis of reinforced concrete structures using ANSYS non-linear concrete model.* Computational Mechanics, New Trends and Applications. S. Idelsohn, E. Oate and E. Dvorkin (Eds.). CIMNE, Barcelona, Spain.

Biddah, Ashraf (2003) *Experimental investigation of pultruded FRP section combined with concrete slab* Paper presented at 6th International Symposium on Fibre-reinforced Polymer Reinforcement for Concrete Structures (FRPRCS-6) July 2003, Singapore

El-Ragaby, A., El-Salakawy, E.F. & Benmokrane, B.(2005) *Finite element modelling of concrete bridge deck slabs reinforced with FRP bars* Proceedings for ACI 7th International Symposium. November 2005. Kansas City. SP230 pp915- 034

Fanning, P. (2001) *Nonlinear models of reinforced and post-tensioned concrete beams* Electronic Journal of Structural Engineering, 2

Girhammar, Ulfrne & Gopu, Vijay K.A. (1993) *Composite beam columns with interlay slip – Exact analysis* Journal of Structural Engineering Vol 119 No 4, pp 1265-1282

Granholm, H (1949). *On composite beams and columns with special regard to nailed timber structures.* Trans. No. 88, Chalmers University of Technology, Goteborg, Sweden

Kachlakev Damien et al. California Polytechnic State University & Miller, Thomas et al. Oregon State University (2001) *Finite element modelling of reinforced concrete structures strengthened with FRP laminates* Final report SPR316 for Oregon Dept of Transport Research Group, Oregon & Federal Highway Administration, Washington DC.

Kang, J. Y, Park, J. S., Park, Y. J. You, Jung, W. T.(2005) *Analytical evaluation of RC beams strengthened with near surface mounted CFRP laminates.* Proceedings for ACI 7th International Symposium. November 2005. Kansas City. SP230 pp915- 034

Newmark, N. M., Seiaa, C. P., and Viest, I. M. (1951). *Tests and analysis of composite beams with incomplete interaction.* Proc., Society of Experimental Stress Analysis, New York, N.Y., Vol. 9, pp 75-92.

Nie, Jianguo & Cai, C.S. (2003) *Steel–concrete composite beams considering shear slip effects* Journal of Structural Engineering Vol 129 No. 4, April 2003 ASCE

Oregon Department of Transport SPR 316 (2001) *Finite element modelling of reinforced concrete structures strengthened with FRP laminates*

Pham, H.B. & Al-Mahaidi, R.(2005) *Finite element modelling of RC beams retrofitted with CFRP fabrics* Proceedings for ACI 7th International Symposium November 2005. Kansas City SP230, pp 499-513.

Pham, H.B. and Al-Mahaidi, R. (2004) *Predicting models for de-bonding failures of CFRP retrofitted concrete beams.* Paper presented at Second International Conference on FRP composites in Civil Engineering, Adelaide, Australia. pp. 531-539.

Queiroz, F. D., Vellasco, P.C.G.S., Nethercroft, D.A.(2006) *Finite element modelling of composite beams with full and partial shear connection* 1st International Conference on Advances in Experimental Structural Engineering (AESE 05), July 2005, Nagoya, Japan, 2005, pp: 959 - 964

Schnabl, S., Planinc, I., Miran, S., Cas, B., Goran, T. (2006) *An analytical model of layered continuous beams with partial interaction* Journal of Structural Engineering and Mechanics, ASCE Vol 22, No.3 March 2006 pp 263-278.

Sen, R., Iyer, M., Issa, M. & Shahawy, M. (1991) *Fibreglass pre-tensioned piles for marine environments.* Proceedings for Advanced Composite Materials in Civil Engineering Structures Conference, November 1991

Yunovich, M., and Thompson, N (2003) *Corrosion of Highway Bridges: Economic Impact and Control Methodologies* Concrete International, American Concrete Institute, Vol.25, No.1. pp.52-57

Kang, J. Y, Park, J. S., Park, Y. J. You, Jung, W. T.(2005) *Analytical evaluation of RC beams strengthened with near surface mounted CFRP laminates.* Proceedings for ACI 7th International Symposium. November 2005. Kansas City. SP230 pp915- 034

الدراسات العملية والنمذجة العددية لقطاعات الألياف الزجاجية والكربونية المهجنة مع البلاطات الخرسانية والمدعمة باستخدام الألياف الكربونية

الخلاصة

ازداد مؤخراً استخدام المواد المركبة من الألياف والبوليمرات في صناعة التشييد على مستوى العالم. المواد المركبة من الألياف والبوليمرات كانت الاختيار الأول منذ الستينات من القرن الماضي في صناعة الطيران والفضاء. ولكن مؤخراً بدأت المواد المركبة من ألياف الزجاج والبوليمرات تكتسب القبول كأحد مواد الانشاء في صناعة التشييد وذلك نظراً لزيادة مقاومتها وصلابتها بالمقارنة إلى وزنها، كذلك مقاومتها العالية للصدأ وسهولة استخدامها. أيضاً المواد المركبة من ألياف الكربون والبوليمرات أصبحت تنافس كأحد مواد الانشاء لما لها من مقاومة تفوق تلك التي للمواد المركبة من ألياف الزجاج والبوليمرات.

هذه الدراسة توضح إلى دراسة امكانية استخدام المواد المركبة من ألياف الزجاج وألياف الكربون والبوليمرات مع بعضها البعض في بعض العناصر الانشائية مثل الكمرات الخرسانية للأستفادة من هذا النظام المزدوج Hybrid System الذي يعطي أدائية وإنشائية عالية بالإضافة إلى خفة الوزن ومقاومة الصدأ.

من أهداف الدراسة هو بحث سلوك القطاعات الخرسانية المركبة المستخدم فيها نظام مزدوج من الألياف تحت تأثير قوى الانحناء. القطاع المركب يتكون من بلاطة خرسانية متصلة بكمرات من المواد المركبة من ألياف الزجاج والبوليمرات مع استخدام شرائح من المواد المركبة من ألياف الكربون والبوليمرات كتسليح حقلي خارجي للبلاطة. ويهدف هذا النظام إلى تعظيم الاستفادة من خواص كل مادة مثل مقاومة الشد العالية لشرائح ألياف الكربون، مقاومة الضغط للخرسانة، خفة الوزن وانخفاض التكلفة للكمرات من ألياف الزجاج بالإضافة إلى مقاومة الصدأ العالية لجميع المكونات.

اشتمل البحث على تصنيع واختبار عدد ثلاث عينات. وقد تم اختبار العينات حتى حدوث الانهيار مع متابعة وتسجيل سهم الانحناء والانفعالات المختلفة. تم إعداد نموذج عددي على الحاسب الآلي باستخدام نظرية العناصر المحددة واستخدام برنامج ANSYS وذلك لتمثيل سلوك الكمرات من خلال مرحلة التحميل المرن لبيان تأثير الاختلافات في المواد وخواصها وذلك من أجل تحديد الاختيار الأمثل لهذه المواد.

أظهرت الدراسة فوائد استخدام قطاعات مركبة من نظام مزدوج من المواد المركبة من الألياف والبوليمرات وكذلك الخرسانة لزيادة قدرة التحمل في الانحناء وكذلك لزيادة الصلابة. كما إن النموذج المستخدم يمكن تطويره للاستخدام في المستقبل مع مواد أخرى حديثة. نتائج هذا البحث تعتبر إضافة لكل من الباحثين والمصممين في مجال استخدام المواد المركبة من الألياف والبوليمرات.

جامعة الإمارات العربية المتحدة
عمادة الدراسات العليا
برنامج ماجستير علوم المواد

الدراسات العملية والنمذجة العددية لقطاعات الألياف الزجاجية والكربونية المهجنة مع البلاطات الخرسانية والمدعمة باستخدام الألياف الكربونية

رسالة مقدمة من الطالب:

أستيفن كريج رينور

تحت إشراف

د. أشرف بده
أستاذ مشارك بقسم الهندسة المدنية و البيئية
كلية الهندسة – جامعة الإمارات العربية المتحدة

د. خالد الصاوى
أستاذ مشارك بقسم الهندسة المدنية و البيئية
كلية الهندسة – جامعة الإمارات العربية المتحدة

إستكمالا لمتطلبات الحصول على درجة الماجستير فى علوم المواد

يونيو ٢٠٠٧